



A suppressor of axillary meristem maturation promotes longevity in flowering plants

Omid Karami¹, Arezoo Rahimi¹, Majid Khan^{1,5}, Marian Bemer², Rashmi R. Hazarika³, Patrick Mak^{1,6}, Monique Compier^{1,7}, Vera van Noort^{3,4} and Remko Offringa^{3,4}✉

Post-embryonic development and longevity of flowering plants are, for a large part, determined by the activity and maturation state of stem cell niches formed in the axils of leaves, the so-called axillary meristems (AMs)^{1,2}. The genes that are associated with AM maturation and underlie the differences between monocarpic (reproduce once and die) annual and the longer-lived polycarpic (reproduce more than once) perennial plants are still largely unknown. Here we identify a new role for the *Arabidopsis* AT-HOOK MOTIF NUCLEAR LOCALIZED 15 (AHL15) gene as a suppressor of AM maturation. Loss of AHL15 function accelerates AM maturation, whereas ectopic expression of AHL15 suppresses AM maturation and promotes longevity in monocarpic *Arabidopsis* and tobacco. Accordingly, in *Arabidopsis* grown under longevity-promoting short-day conditions, or in polycarpic *Arabidopsis lyrata*, expression of AHL15 is upregulated in AMs. Together, our results indicate that AHL15 and other AHL clade-A genes play an important role, directly downstream of flowering genes (SOC1, FUL) and upstream of the flowering-promoting hormone gibberellic acid, in suppressing AM maturation and extending the plant's lifespan.

Plant architecture and longevity are dependent on the activity of stem cell groups called meristems. The primary shoot and root apical meristem of a plant are established during early embryogenesis and give rise, respectively, to the shoot and the root system during post-embryonic development. In flowering plants, post-embryonic shoot development begins with a vegetative phase during which the primary shoot apical meristem (SAM) produces morphogenetic units called phytomers consisting of a stem (internode) subtending a node with a leaf and a secondary or axillary meristem (AM) located in the axil of the leaf^{1,2}. Both the SAM and these AMs undergo a maturation process. Like the SAM, young immature AMs are vegetative and, when activated, they produce leaves whereas in plant species such as *Arabidopsis thaliana* (*Arabidopsis*) partially matured AMs produce a few cauline leaves before they fully mature into inflorescence meristems and start developing phytomers comprising a stem subtending one or more flowers^{2,3}.

The maintenance of vegetative development after flowering is an important determinant of plant longevity and life history. Monocarpic plants, such as the annuals *Arabidopsis* and *Nicotiana tabacum* (tobacco), complete their life cycle in a single growing season. The AMs that are established during the vegetative phase initially produce leaves. Following floral transition, however, all AMs

rapidly convert into inflorescence meristems producing secondary and tertiary inflorescences with bracts and flowers, thus maximizing offspring production before the plant's life ends with senescence and death. The number of leaves and bracts produced by an AM is thus a measure of its maturation state following activation. By contrast, many other flowering plant species are polycarpic perennials, such as the close *Arabidopsis* relative *A. lyrata*. Under permissive growth conditions, these can live and flower for more than two growing seasons. Because some AMs are maintained in the vegetative state, this allows polycarpic plants to produce new shoots after seed set and the subsequent activation of these AMs by appropriate growth conditions before the start of the next growing season^{4,5}. Despite considerable interest in the molecular basis of plant life history, the proposed molecular mechanisms determining the difference in loss or maintenance of vegetative development after flowering between, respectively, monocarpic and polycarpic plants are still largely based on our extensive knowledge on the control of flowering in *Arabidopsis* and closely related species. From these studies, the MADS box proteins SUPPRESSOR OF OVEREXPRESSION OF CONSTANS 1 (SOC1) and FRUITFULL (FUL) have been identified as key promoters of flowering and monocarpic growth, and FLOWERING LOCUS C (FLC) as their upstream cold-sensitive inhibitor⁶⁻⁷. However, the factors that maintain vegetative development after flowering, and thereby allow polycarpic growth, remain elusive.

Here we present evidence that the *Arabidopsis* gene AT-HOOK MOTIF NUCLEAR LOCALIZED 15 (AHL15) plays an important role in the control of AM maturation and extending the plant's lifespan. This gene forms a clade (clade A) with 14 other AHL genes in *Arabidopsis* that encode nuclear proteins containing a single N-terminal DNA-binding AT-hook motif and a C-terminal plants and prokaryotes conserved (PPC) domain (Supplementary Fig. 1a). The PPC domain was previously shown to contribute to physical interaction with other AHL or nuclear proteins⁸. AHL15 homologues have been implicated in several aspects of plant growth and development in *Arabidopsis*, including hypocotyl growth and leaf senescence⁸⁻¹⁰, flower development¹¹ and flowering time^{10,12}.

In contrast to other *ahl* mutants¹⁰, *ahl15* loss-of-function mutant plants (Supplementary Fig. 1b–e) flowered at the same time and developed the same number of rosette leaves before flowering as wild-type plants, under both short-day (SD) and long-day (LD) conditions (Extended Data Fig. 1d,e). After bolting, however, AMs located in the axils of rosette leaves (rosette AMs) of *ahl15* mutant

¹Plant Developmental Genetics, Institute of Biology Leiden, Leiden University, Leiden, the Netherlands. ²Laboratory of Molecular Biology and B.U. Bioscience, Wageningen University and Research, Wageningen, the Netherlands. ³KU Leuven, Centre of Microbial and Plant Genetics, Leuven, Belgium. ⁴Bioinformatics and Genomics, Institute of Biology Leiden, Leiden University, Leiden, the Netherlands. ⁵Present address: Institute of Biotechnology and Genetic Engineering, University of Agriculture Peshawar, Peshawar, Pakistan. ⁶Present address: Sanquin Plasma Products BV, Department of Product Development, Amsterdam, the Netherlands. ⁷Present address: Rijk Zwaan, De Lier, the Netherlands. ✉e-mail: r.offringa@biology.leidenuniv.nl

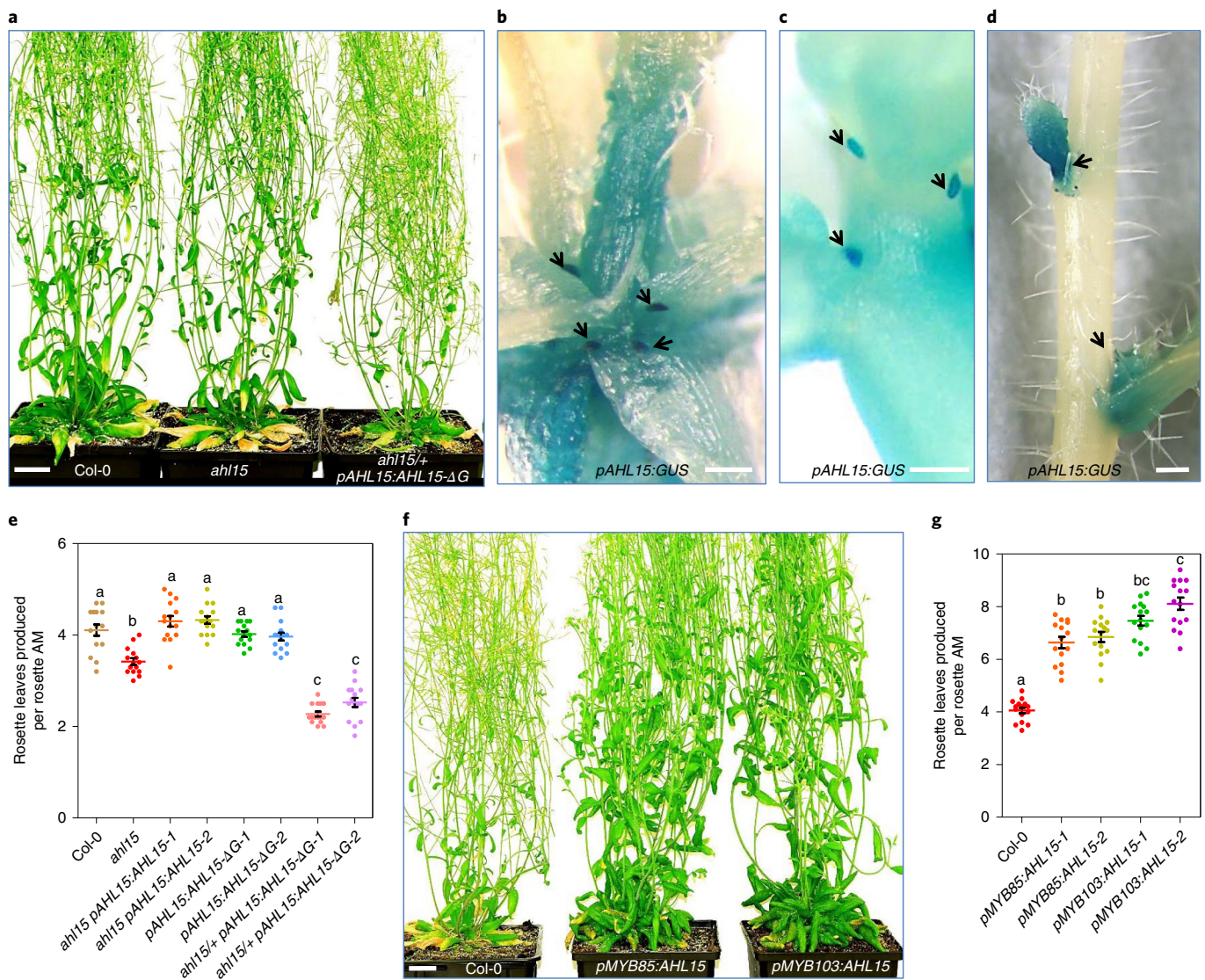


Fig. 1 | AHL15 represses AM maturation in Arabidopsis. **a**, Shoot phenotypes of 50-day-old flowering wild-type (left), *ah15* (middle) and *ah15/+ pAHL15:AHL15-ΔG* mutant (right) plants. **b-d**, *pAHL15:GUS* expression in rosette AMs (arrowheads in **b**), in aerial AMs located on a young inflorescence stem (arrowheads in **c**) and in activated axillary buds on an inflorescence stem (arrowheads in **d**) of a flowering plant. **e**, Rosette leaves produced per rosette AM in 50-day-old wild-type, *ah15*, *ah15 pAHL15:AHL15*, *pAHL15:AHL15-ΔG* and *ah15/+ pAHL15:AHL15-ΔG* plants. **f**, Shoot phenotype of a 60-day-old flowering wild-type (left), *pMYB85:AHL15* (middle) and *pMYB103:AHL15* (right) plant. **g**, Rosette leaves produced per rosette AM in 60-day-old wild-type, *pMYB85:AHL15* and *pMYB103:AHL15* plants. Coloured dots in **e,g** indicate the number of rosette leaves per plant ($n=15$ biologically independent plants) per line, horizontal lines indicate the mean and error bars indicate s.e.m. **e,g**, Different letters indicate statistically significant differences ($P < 0.01$) as determined by one-way analysis of variance with Tukey's honest significant difference post hoc test. *P* values are provided in Supplementary Tables 3 and 4. Plants were grown under LD conditions. Scale bars, 2 cm in **a,f** and 1 mm in **b,c**. Leaf production per rosette AM in **e,g** was determined for two independent transgenic lines (1 and 2). For **a,f**, similar results were obtained from three independent experiments. For **b-d**, similar results were obtained from two independent experiments.

plants produced fewer additional rosette leaves compared to those in wild-type plants (Fig. 1a,e and Extended Data Fig. 2a–c). More detailed analysis showed that this reduction in additional rosette leaf production in *ah15* plants was caused neither by delayed outgrowth of rosette AMs into axillary buds nor by early floral transition, but rather by a reduction in the vegetative activity of these buds (Extended Data Fig. 3a,b). Following floral transition, *ah15* rosette AMs produced the same number of cauline leaves (Extended Data Fig. 2d) and flowers (Supplementary Fig. 2a) as the wild type (Col-0). However, the cauline branches produced by aerial AMs on *ah15* inflorescences developed fewer cauline leaves (Extended Data Fig. 2e) and flowers/fruits (Supplementary Fig. 2b)

compared to those produced by wild-type inflorescences, resulting in a significant reduction in the total number of cauline leaves and flowers on *ah15* inflorescences. Introduction of the *pAHL15:AHL15* genomic clone into the *ah15* mutant background restored both the rosette and cauline leaf, as well as flower and fruit numbers to wild-type levels (Fig. 1e, Extended Data Fig. 2a–e and Supplementary Fig. 2b), confirming that the phenotypes resulted from *ah15* loss-of-function. β -Glucuronidase (GUS) staining of plants carrying a *pAHL15:GUS* promoter–reporter fusion showed that *AHL15* is expressed in AMs (Fig. 1b,c) and young axillary buds (Fig. 1d). Together these results suggested a novel role for *AHL15* in controlling AM maturation.

AHL proteins interact with each other through their PPC domain, and with other non-AHL proteins through a conserved six-amino acid (GRFEIL) region in the PPC domain. Expression of an AHL protein without the GRFEIL region leads to a dominant negative effect, because it generates a non-functional complex that is unable to modulate transcription⁸. Expression of a deletion version of AHL15 lacking the GRFEIL region under control of the *AHL15* promoter (*pAHL15:AHL15-ΔG*) in the wild-type background ($n=20$) resulted in fertile plants (Extended Data Fig. 1a,b) showing normal AM maturation (Fig. 1e and Extended Data Fig. 2). In the heterozygous *ahl15* loss-of-function background, however, *pAHL15:AHL15-ΔG* expression induced early flowering (Extended Data Figs. 1d,e and 3b), resulting in a strong reduction in rosette and cauline leaf production by AMs (Fig. 1a,e and Extended Data Figs. 2a–f and 3a). Homozygous *ahl15 pAHL15:AHL15-ΔG* progeny were not obtained, and the presence of defective seeds in siliques of *ahl15/+ pAHL15:AHL15-ΔG* plants suggests that this genetic combination is embryo lethal (Extended Data Fig. 1b,c). The much stronger phenotypes observed for *ahl15/+ pAHL15:AHL15-ΔG* plants are in line with the dominant negative effect of *AHL15-ΔG* expression, overcoming functional redundancy among *Arabidopsis* clade-A AHL family members^{8–10}.

Based on the observation that the flowering time and number of rosette leaves before bolting were the same for both wild-type and *ahl15* loss-of-function plants, but not for *ahl15/+ pAHL15:AHL15-ΔG* plants, we speculated that other AHL clade-A family members are more active in the SAM, whereas *AHL15* acts more strongly on AM maturation. To test this, we overexpressed a fusion protein between *AHL15* and the rat glucocorticoid receptor under control of the constitutive cauliflower mosaic virus 35S promoter (*p35S:AHL15-GR*). This rendered the nuclear import, and thereby the activity of the ectopically expressed *AHL15-GR* fusion, inducible by dexamethasone (DEX). Untreated *p35S:AHL15-GR* plants showed a wild-type phenotype (Extended Data Fig. 4b,c) but, after spraying flowering *p35S:AHL15-GR* plants with DEX, rosette AMs produced significantly more rosette and cauline leaves (Extended Data Fig. 4a–c). Interestingly, spraying *p35S:AHL15-GR* plants before flowering also significantly delayed their floral transition (Extended Data Fig. 4d), indicating that ectopically expressed *AHL15* can also suppress maturation of the SAM. In turn, overexpression of the *Arabidopsis* AHL family members *AHL19*, *AHL20*, *AHL27* and *AHL29*, as well as the putative *AHL15* orthologues from *Brassica oleracea* and *Medicago truncatula* in *Arabidopsis*, resulted in morphological changes similar to those observed for *p35S:AHL15-GR* plants after DEX treatment. The overexpression plants produced more rosette and cauline leaves during flowering (Extended Data Fig. 5), supporting the idea that there is functional redundancy among AHL clade-A family members and that the ability to control either SAM or AM maturation is dependent on the spatio-temporal expression of the corresponding genes.

In contrast to the observed growth arrest and death of 2-month-old *Arabidopsis* plants grown under LD conditions (Fig. 2d), 4-month-old SD *Arabidopsis* plants continued to grow after the first cycle of flowering because aerial AMs on the last-formed lateral branches produced new rosette leaves (Fig. 2a and Extended Data Fig. 6). However, SD *ahl15* mutant plants did not show this renewed vegetative growth and died, whereas *ahl15 pAHL15:AHL15* plants grew like the wild type under these conditions (Fig. 2a and Extended Data Fig. 6). GUS staining of *pAHL15:GUS* plants revealed that *AHL15* expression was strongly enhanced in young lateral inflorescences, axils of cauline leaves and rosette branches under SD conditions compared to LD conditions (Fig. 2b,c and Extended Data Fig. 7), indicating that *AHL15* expression is day length sensitive and confirming the important role of this gene in extending the lifespan of *Arabidopsis* under SD conditions.

Growing *Arabidopsis* plants under SD conditions significantly delays flowering¹³, and this might thus indirectly enhance the repressive effect of *AHL15* on AM maturation and extend the lifespan. To assess *AHL15* function independently of day length and flowering time, we expressed *AHL15* under the control of promoters *pMYB85* or *pMYB103*, which are highly active in *Arabidopsis* rosette nodes and aerial axillary buds (Extended Data Fig. 8a)¹⁴. Under LD conditions, *pMYB85:AHL15* and *pMYB103:AHL15* plants flowered at the same time as wild-type plants, but their AMs produced significantly more rosette and cauline leaves compared to those in wild-type plants (Fig. 1f,g and Extended Data Fig. 8b,c). Moreover, after flowering and seed set, when wild-type plants senesced and died, *pMYB85:AHL15* and *pMYB103:AHL15* rosette and aerial AMs produced new rosette leaves, which allowed these plants to continue to grow and generate new flowers and seeds (Fig. 2d,e). In addition, senesced *p35S:AHL15-GR* plants carrying fully ripened siliques began new aerial vegetative development on lateral secondary inflorescences after DEX treatment, and ultimately produced new inflorescences from the resulting rosettes (Extended Data Fig. 9a). Interestingly, the development of vegetative shoots from AMs formed on rosette and aerial nodes after reproduction also contributes to the polycarpic growth habit of *Arabis alpina* and *Cardamine flexuosa* plants^{15,16}. Our results indicate that increased expression of *AHL15* in the late stages of development promotes longevity by inducing a polycarpic-like growth habit in *Arabidopsis*, with an important difference that AMs remaining vegetative do not show dormancy.

To determine whether heterologous *AHL15* expression could induce similar developmental changes in a monocarpic plant species from a different family, we introduced the *35S:AHL15-GR* construct into tobacco. Wild-type and *p35S:AHL15-GR* tobacco plants were allowed to grow and set seeds in the absence of DEX treatment. After seed harvesting, all leaves and side branches were removed and the bare lower parts of the primary stems were either mock or DEX treated. Whereas stems of wild-type and mock-treated *p35S:AHL15-GR* plants did not show any growth, AMs on DEX-treated *p35S:AHL15-GR* tobacco stems resumed vegetative growth, eventually leading to a second cycle of flowering and seed set (Fig. 2f). Continued DEX treatment after each subsequent cycle of seed harvesting efficiently induced vegetative growth and subsequent flowering and seed set, allowing *p35S:AHL15-GR* tobacco plants to survive at least 3 years (Extended Data Fig. 9b). This result confirmed the conclusion from previous overexpression experiments (Fig. 2d,e and Extended Data Figs. 4 and 9a) that enhanced *AHL15* expression facilitates polycarpic-like growth by maintaining some AMs in the vegetative state after flowering.

Previously, loss of function of both *SOC1* and *FUL* in *Arabidopsis* was reported to suppress AM maturation, resulting in polycarpic-like growth⁶. We found that the aerial rosette formation normally observed in the *soc1 ful* double mutant was significantly reduced in *soc1 ful ahl15* triple-mutant plants (Fig. 3a,b). Moreover, polycarpic features of the *soc1 ful* double mutant were lost in the *ahl15* mutant background because *soc1 ful ahl15* plants senesced and died following seed set, just like wild-type *Arabidopsis*. Expression analysis by quantitative PCR (qPCR) with reverse transcription (Fig. 3c), or by using the *pAHL15:GUS* reporter (Fig. 3d,e), showed that *AHL15* was indeed strongly upregulated in *soc1 ful* inflorescence nodes and lateral inflorescences. Previous studies have revealed that the expression of *SOC1* is positively regulated by LD conditions. Moreover, *SOC1* was shown to bind to the *AHL15* upstream and downstream regions (Chr3, 20603158–20604316 and 20610947–20612012), which both contain a canonical CARG-box (CC[A/T]6GG) (Fig. 3f)^{17–19}. This, together with our own data, suggested that *AHL15* expression is repressed by *SOC1* under LD conditions (Fig. 2c) and that unrepressed *AHL15* activity in the *soc1 ful* background explains the aerial rosette formation and

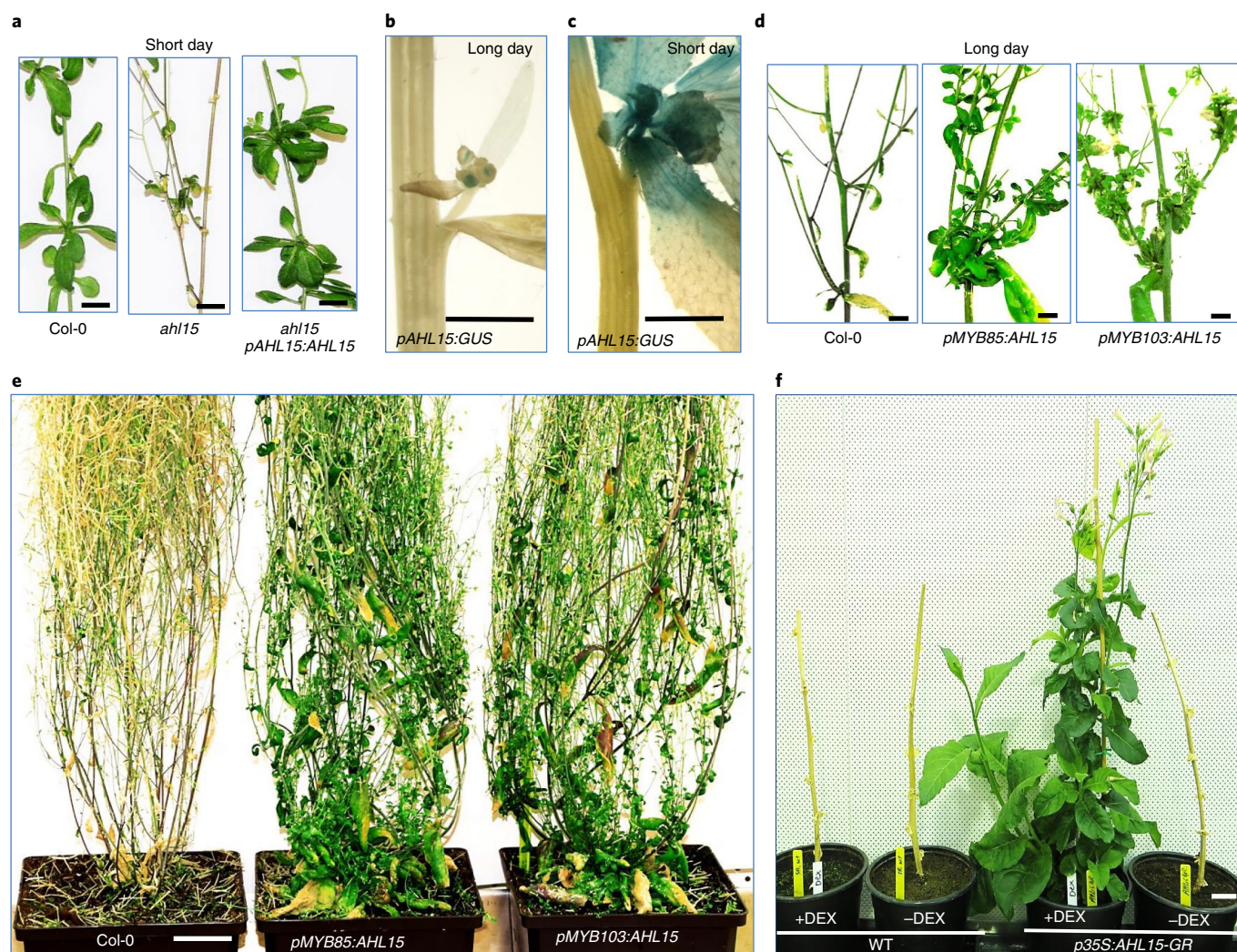


Fig. 2 | *AHL15* promotes longevity in *Arabidopsis* and tobacco. **a, Rosette leaves produced by aerial AMs in 4-month-old wild-type (left) and *ah15* *pAHL15:AHL15* (right) plants, but not in *ah15* mutant plants (middle), grown under SD conditions. **b,c**, *pAHL15:GUS* expression in a lateral inflorescence of a 9-week-old plant grown under LD conditions (**b**) and a 4-month-old plant grown under SD conditions (**c**). **d**, Lateral aerial nodes without and with rosette leaves in 4-month-old wild-type (left), *pMYB85:AHL15* (middle) and *pMYB103:AHL15* (right) plants grown under LD conditions. **e**, Phenotype of 4-month-old wild-type (Col-0, left), *pMYB85:AHL15* (middle) and *pMYB103:AHL15* (right) plants grown under LD conditions. **f**, Growth response of 5-month-old wild-type (WT, left) and *35S:AHL15-GR* (right) tobacco plants grown under LD conditions. Scale bars, 1 cm in **a-d**, 2 cm in **b** and 5 cm in **c**. **a-c,f**, Similar results were obtained from two independent experiments. **d,e**, Similar results were obtained from three independent experiments.**

polycarpic-like growth of mutant plants. To check whether the CarG-box-containing regions could also be bound by FUL, we used stem fragments containing axillary nodes of *pFUL:FUL-GFP ful* plants to perform chromatin immunoprecipitation (ChIP). Subsequent qPCR revealed significant enrichment for both upstream and downstream regions (Fig. 3g), indicating that FUL can repress *AHL15* expression by direct binding to these regions. To further confirm that FUL and SOC1 can bind CarG-boxes in the *AHL15* up- and downstream regions, we performed electrophoretic mobility shift assay (EMSA) experiments. Probe fragments containing the corresponding regulatory regions (frag 1 and frag 3), or these regions with a mutated CarG-box (frags 1 m and 3 m), were tested with SOC1 and FUL homo- and heterodimers. The SOC1/FUL heterodimer could bind to both regulatory fragments, but binding was reduced when the CarG-box was mutated in frag 1 m and even completely abolished in frag 3 m (Fig. 3h), providing additional evidence for the importance of the CarG-boxes in regard to the binding of SOC1 and FUL. The SOC1

homodimer showed the same results, while the FUL homodimer did not show binding (Supplementary Fig. 3).

SOC1 and FUL are known as central floral integrators, because they integrate the different environmental and endogenous signalling pathways that influence flowering^{13,17,20}. They promote flowering through activation of the floral meristem genes *APETALA1* (*API*) and *LEAFY* (*LFY*)^{21,22}, and of genes involved in the biosynthesis of the plant hormone gibberellic acid (GA)²³, which plays an important role in the promotion of flowering through activation of *SOC1* and the *SQUAMOSA PROMOTER BINDING PROTEIN-LIKE* (*SPL*) genes^{24,25}. Interestingly, *AHL15* and *AHL25* also control GA biosynthesis by direct binding to the promoter of *GA3-oxidase1* (*GA3OX1*), which encodes an enzyme required for GA biosynthesis²⁶. We therefore investigated the relationship between GA biosynthesis and *AHL15* in the control of AM maturation. qPCR analysis showed that the expression of genes *GA3OX1*, *GA20OX1* and *GA20OX2*, encoding rate-limiting enzymes in the final steps of the GA biosynthetic pathway^{23,27,28},

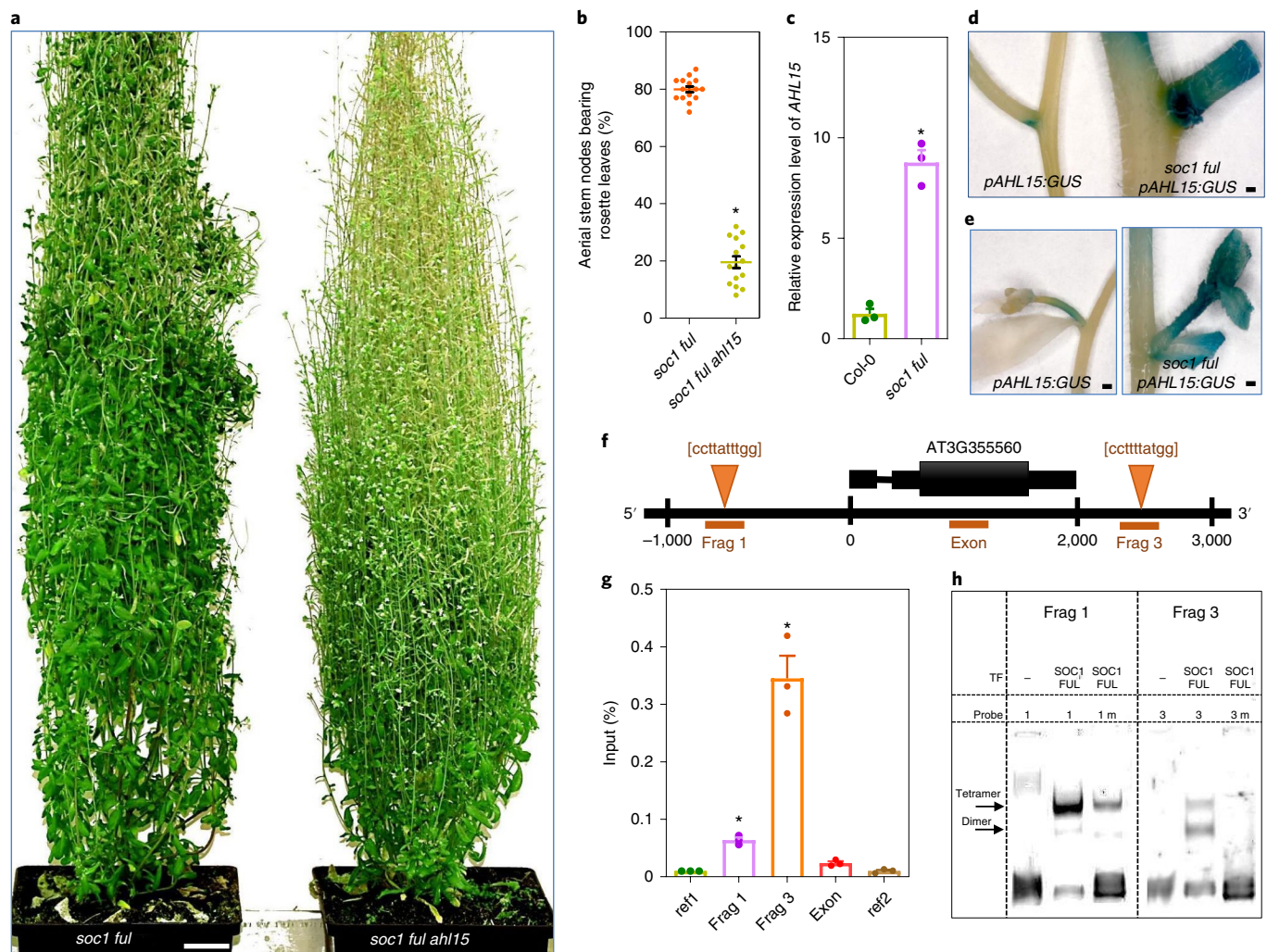


Fig. 3 | *AHL15* is essential for suppression of AM maturation in the *Arabidopsis soc1 ful* mutant. **a**, A 3-month-old *soc1 ful* double-mutant plant with numerous aerial rosettes (left) and a *soc1 ful ah115* triple-mutant plant with a limited number of aerial rosettes (right), both grown under LD conditions. Similar results were obtained from two independent experiments. **b**, Percentage of aerial stem nodes bearing rosette leaves in 3-month-old *soc1 ful* and *soc1 ful ah115* plants. Dots indicate the percentage per plant ($n = 10$ biologically independent plants), horizontal lines the mean and error bars indicate s.e.m. The asterisk indicates a significant difference ($P < 0.001$) as determined by two-sided Student's *t*-test. **c**, qPCR analysis of *AHL15* expression in secondary inflorescence nodes of wild-type (Col-0) and *soc1 ful* plants 2 weeks after flowering. Dots indicate the values of three biological replicates per plant line, bars indicate the mean and error bars indicate s.e.m. The asterisk indicates a significant difference ($P < 0.001$) as determined by two-sided Student's *t*-test. **d, e**, *pAHL15:GUS* expression in an inflorescence node (**d**) and a secondary inflorescence (**e**) in wild-type (left) or a *soc1 ful* mutant (right) background. Plants were at a comparable developmental stage, and similar results were obtained from two independent experiments. **f**, *AHL15* gene model with canonical CARG-boxes located in the upstream (frag 1) and downstream (frag 3) regions, but not in the exon fragment that was used as control (exon). The *AHL15* coding region is indicated by a thick black bar, exons by intermediate black bars and the position of the intron by a black line. **g**, Graph showing ChIP-qPCR results from *FUL-GFP ap1 cal* secondary inflorescence nodes using an anti-green fluorescent protein antibody. Enrichment of fragments was calculated as a percentage of the input sample. ref1 and ref2 are reference fragments (see Methods), while other fragments are also indicated in the gene model. Dots indicate the values of three biological replicates, bars the means and error bars indicate s.e.m. Asterisks indicate significant differences with ref1 and ref2 ($P < 0.001$) as determined by two-sided Student's *t*-test. Exact *P* values are provided in Supplementary Table 5. **h**, Binding of the transcription factors (TFs) SOC1 and FUL to regulatory regions near *AHL15*. Left: EMSA of promoter frag 1 with a wild-type (1) or mutated (m1) CARG-box. Right: EMSA of downstream frag 3 with a wild-type (3) or mutated (3m) CARG-box. Shifting of the probe, indicating binding, occurred through either a tetramer (top band) or dimer (bottom band). Similar results were obtained from two independent experiments. Scale bars, 2 cm in **a** and 1 mm in **d, e**.

was downregulated in DEX-treated *35S:AHL15-GR* inflorescence nodes (Fig. 4a). In line with the downregulation of GA biosynthesis, GA application to DEX-treated flowering *p35S:AHL15-GR* plants resulted in marked repression of vegetative AM activity (Fig. 4b). In turn, treatment of flowering wild-type *Arabidopsis* plants by paclobutrazol, a potent inhibitor of GA biosynthesis, prevented AM maturation, resulting in aerial rosette leaf formation and enhanced longevity (Fig. 4c). Based on our findings,

we postulate that *AHL15* acts downstream of SOC1 and FUL as a central repressor of AM maturation, and that *AHL15* prevents AM maturation in part by suppressing GA biosynthesis (Fig. 4d). Interestingly, the polycarpic behaviour of *A. alpina* was shown to be based on age-dependent suppression of *AaSOC1* expression¹⁵ and GA levels²⁹ and, as in our model (Fig. 4d), *AHL* genes may also link these two regulatory pathways thus facilitating polycarpic growth in *A. alpina*.

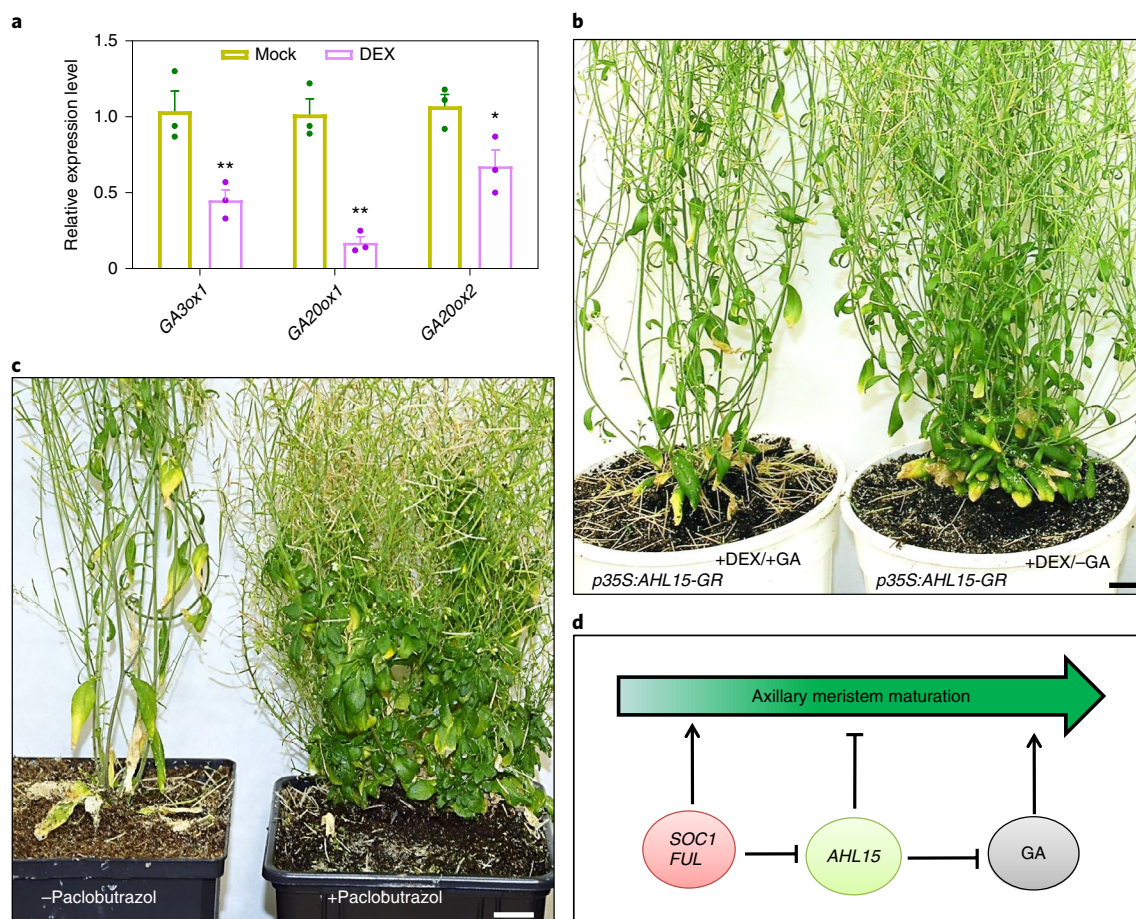


Fig. 4 | AHL15 delays AM maturation in part by suppression of GA biosynthesis. **a**, Relative expression level of GA biosynthesis genes *GA3OX1*, *GA20OX1* and *GA20OX2* by qPCR analysis in the basal regions of 1-week-old *35S:AHL15-GR* inflorescences 1 day after spraying with either water (mock) or 20 μM DEX. Dots indicate the values of three biological replicates per plant line, bars indicate the mean and error bars indicate s.e.m. Asterisks indicate significant differences from mock-treated plants ($*P < 0.05$, $**P < 0.01$), as determined by two-sided Student's *t*-test. **b**, Shoot phenotype of 3-month-old *p35S:AHL15-GR* plants that were DEX sprayed at 5 weeks of age and subsequently sprayed 1 week later with either 10 μM GA_4 (+GA) or water (-GA). Similar results were obtained from two independent experiments. **c**, Shoot phenotype of 3-month-old wild-type *Arabidopsis* plants that were sprayed 6 weeks earlier with either water (-Paclobutrazol) or 3 μM paclobutrazol (+Paclobutrazol). Similar results were obtained from two independent experiments. Plants in **b,c** were grown under LD conditions; scale bars, 2 cm. **d**, Proposed model for the key role of *AHL15* (and other *AHL* clade-A genes) in controlling AM maturation downstream of flowering genes *SOC1* and *FUL* and upstream of GA biosynthesis. Blunt-ending lines indicate repression, arrows indicate promotion.

The existence of both mono- and polycarpic species within many plant genera indicates that life history traits have changed frequently during evolution⁵. *AHL* clade-A gene families can be found in both mono- and polycarpic plant species (Supplementary Fig. 4a)³⁰, and expression of the *AHL* clade-A gene family could therefore provide a mechanism by which a plant species attains a polycarpic growth habit. Comparison of gene family size in representative species of three plant families did, however, not show obvious gene deletion or duplication events linked, respectively, to the mono- or polycarpic growth habit (Supplementary Fig. 4b). This suggests that a switch from mono- to polycarpic habit or vice versa could possibly be mediated by a change in gene regulation.

To find support for this, we compared the *AHL* gene family of *Arabidopsis* with that of its close polycarpic relative *A. lyrata*³¹. The *Arabidopsis* and *A. lyrata* genomes both encode 15 *AHL* clade-A proteins, among which orthologous pairs can clearly be identified based on amino acid sequence identity (Supplementary Fig. 5). We hypothesized that the polycarpic habit of *A. lyrata* might be associated with enhanced *AHL* clade-A gene expression leading to the maintenance of basal AMs in the vegetative state

during flowering (Extended Data Fig. 10a). Analysis of individual *AHL* clade-A genes in *Arabidopsis* showed that expression of the majority of these genes, including *AHL15*, *AHL19* and *AHL20*, was decreased in rosette nodes of *Arabidopsis* flowering plants compared with 2-week-old seedlings (Extended Data Fig. 10b). In contrast, the expression of five members of the *AHL* gene family (*AHL15*, *AHL17*, *AHL19*, *AHL20* and *AHL27*) was significantly higher in rosette nodes of flowering *A. lyrata* plants compared with seedlings (Extended Data Fig. 10c). These data are in line with our hypothesis, and suggest that the different life history strategies in *Arabidopsis* and *A. lyrata* may be associated with the differential regulation of *AHL* genes in AMs.

In conclusion, our data provide evidence for a novel role for *AHL15* and other *AHL* clade-A genes in suppression of AM maturation and enhancement of plant longevity. *Arabidopsis* plants with enhanced *AHL15* expression show polycarpic-like growth, but their vegetative AMs lack the dormancy that is characteristic of reproductive cycles in perennial plants (for example, *A. lyrata* and *A. alpina*). The importance of the *SOC1/FUL*–*AHL*–*GA* pathway in perennial life history therefore requires further confirmation. Although the

exact mode of action of AHL proteins is largely unknown, they are characterized as DNA-binding proteins and, like AT-hook proteins in animals, they seem to act through chromatin remodelling^{11,32}. It has been shown that AHL22 represses *FLOWERING LOCUS T* (*FT*) expression by binding to the *FT* promoter, where it possibly modulates the epigenetic signature around its binding region¹². Detailed studies on the chromatin configuration by approaches, such as chromosome conformation capture technologies³³, should provide more insight into the mode of action of these plant-specific AT-hook motif proteins. One of the objectives of our future research will be to unravel the molecular mechanisms by which these proteins influence plant development.

Methods

Plant materials, growth conditions and phenotyping. All *Arabidopsis* mutant and transgenic lines used in this study were in a Columbia (Col-0) background. The *ahl15* (SALK_040729) transfer DNA (tDNA) insertion mutant and the previously described *soc1-6 ful-7* double mutant³⁴ were obtained from the Nottingham *Arabidopsis* Stock Centre. Seeds were planted directly into soil in pots and germinated at 21 °C, 65% relative humidity and a 16- (LD) or 8-h (SD) photoperiod. When seedlings were 10 d old, they were thinned to one seedling per pot by cutting the hypocotyls. To score for phenotypes including longevity, Col-0 wild-type, mutant or transgenic plants were transferred to larger pots about 3 weeks after flowering. *N. tabacum* cv SR1 Petit Havana (tobacco) plants were grown in medium-sized pots at 25 °C, 70% relative humidity and a 16-h photoperiod. In regard to DEX (Sigma-Aldrich) treatment, *Arabidopsis* and tobacco plants were sprayed with 20 or 30 μM DEX, respectively. To test the effect of GA on AHL15-GR activation by DEX treatment, 35-d-old flowering *p35S::AHL15-GR* plants were first sprayed with 20 μM DEX followed 1 week later by spraying with 10 μM GA4 (Sigma-Aldrich). The production of rosette leaves, cauline leaves, flowers or fruits per rosette or aerial AM of 5-, 7-, 9- or 10-week-old plants was determined by dividing the total number of leaves or fruits produced by the number of active rosette or aerial AMs per plant. In regard to flowering time, the number of rosette leaves produced by the SAM was counted following bolting.

Plasmid construction and transgenic *Arabidopsis* lines. To generate the different promoter:*AHL15* gene fusions, the complete *AHL15* (AT3G55560) genomic fragment from ATG to stop codon was amplified from genomic DNA of *Arabidopsis* ecotype Columbia (Col-0) using PCR primers Gateway-AHL15-F and -R (Supplementary Table 1). The resulting fragment was inserted into pDONR207 via a BP reaction. LR reactions were carried out to fuse the *AHL15* coding region downstream of the 35S promoter in destination vector pMDC32 (ref. ³⁵). Subsequently, the 35S promoter was excised with *KpnI* and *SphI* and replaced by the Gateway cassette (*ccdB* flanked by *attP* sequences) amplified from pMDC164 (ref. ³⁵) by the *KpnI* and *SphI* flanked primers (Supplementary Table 1), resulting in plasmid pGW-AHL15. To generate the constructs *pFD::AHL15*, *pMYB85::AHL15*, *pMYB103::AHL15* and *pAHL15::AHL15*, 3-kb regions upstream of the ATG start codon of genes *FD* (AT4G35900), *MYB85* (AT4G22680), *MYB103* (AT1G63910) and *AHL15* were amplified from ecotype Columbia (Col-0) gDNA using the forward (F) and reverse (R) PCR primers indicated in Supplementary Table 1. The resulting fragments were first inserted into pDONR207 by BP reaction, and subsequently cloned upstream of the *AHL15* genomic fragment in destination vector pGW-AHL15 by LR reaction. To generate reporter constructs *pAHL15::GUS*, *pMYB85::GUS* and *pMYB103::GUS*, the corresponding promoter fragments were cloned upstream of the *GUS* gene in destination vector pMDC164 by LR reaction. To generate the *pAHL15::AHL15-ΔG* construct, a synthetic *KpnI-SpeI* fragment containing the *AHL15* coding region lacking the sequence encoding amino acids Gly-Arg-Phe-Glu-Ile-Leu in the C-terminal region (BaseClear) was used to replace the corresponding coding region in the *pAHL15::AHL15* construct. To construct *35S::AHL15-GR*, a synthetic *PstI-XhoI* fragment containing the *AHL15-GR* fusion (Shine Gene Molecular Biotech; see Supplementary File 1) was used to replace the *BBM-GR* fragment in binary vector pSRS031 (ref. ³⁶). To generate the remaining overexpression constructs, full-length complementary DNA clones of *AHL19* (AT3G04570), *AHL20* (AT4G14465), *AHL27* (AT1G20900) and *AHL29* (AT1G76500) from *Arabidopsis* Col-0, *AC129090* from *M. trunculata* cv Jemalong (*MtAHL15*) and *Bo-Hook1* (*AM057906*) from *B. oleracea* var *cv glabrala* (*BoAHL15*) were used to amplify the open reading frames using the primers indicated in Supplementary Table 1. The resulting fragments were cloned into plasmid pJET1/blunt (GeneE PCR Cloning Kit, no. K1221), and subsequently transferred as *NotI* fragments to binary vector pGPTV 35S-FLAG³⁷. All binary vectors were introduced into *Agrobacterium tumefaciens* strain AGL1 by electroporation³⁸, and *Arabidopsis* Col-0 and *ahl15* plants were transformed using the floral dip method³⁹.

Tobacco transformation. Round leaf discs were prepared from the lamina of the third and fourth leaves of 1-month-old, soil-grown tobacco plants. The leaf discs

were surface sterilized by three washes with sterile water followed by incubation in 10% chlorine solution for 20 min, and by four or five subsequent washes with sterile water⁴⁰. The surface-sterilized leaf discs were syringe infiltrated with an overnight acetosyringone (AS)-induced culture of *A. tumefaciens* strain AGL1 containing binary vector pSRS031 (grown to OD₆₀₀ = 0.6 in the presence of 100 μM AS) carrying the 35S::*AHL15-GR* construct, and co-cultivated for 3 d in the dark on co-cultivation medium (CCM) consisting of full-strength MS medium⁴¹ with 3% (w/v) sucrose (pH 5.8) solidified with 0.8% (w/v) Diachin agar and supplemented with 2 mg l⁻¹ of 6-benzylaminopurine, 0.2 mg l⁻¹ of 1-naphthaleneacetic acid and 40 mg l⁻¹ of AS. After co-cultivation, the explants were transferred to CCM supplemented with 15 mg l⁻¹ of phosphinothricin (ppt) for selection and 500 mg l⁻¹ of cefotaxime to kill *Agrobacterium*. Regeneration was carried out at 24 °C in a 16-h photoperiod. The regenerated transgenic shoots were rooted in large jars containing 100 ml of hormone-free MS medium with 15 mg l⁻¹ of ppt and 500 mg l⁻¹ of cefotaxime. The rooted transgenic plants were transferred to soil and grown in a growth room at 25 °C, 75% relative humidity and a 16-h photoperiod. All transgenic plants were checked for the presence of the tDNA insert by PCR, using genomic DNA extracted from leaf tissues by the cetyltrimethylammonium bromide method⁴².

Histochemical staining and microscopy. Histochemical staining of transgenic lines for GUS activity was performed as described previously⁴³. Tissues were stained for 4 h at 37 °C, followed by chlorophyll extraction and rehydration by incubation for 10 min in a graded ethanol series (75, 50 and 25%). GUS-stained tissues were observed and photographed using a Leica MZ12 microscope equipped with a Leica DC500 camera.

qPCR analysis. RNA isolation was performed using a NucleoSpin RNA Plant kit (Macherey-Nagel). For qPCR analysis, 1 μg of total RNA was used for cDNA synthesis with the iScript cDNA Synthesis Kit (BioRad). PCR was performed using the SYBR-Green PCR Master mix (SYBR Premix Ex Taq, Takara) and a CFX96 thermal cycler (BioRad). The Pfaffl method was used to determine relative expression levels⁴⁴. Expression was normalized using *β-TUBULIN-6* and *EF1-ALPHA* as reference genes. Three biological replicates were performed, with three technical replicates each. The primers used are described in Supplementary Table 2.

ChIP-qPCR experiment. For ChIP-qPCR analysis, three independent samples were harvested from secondary inflorescence nodes of *pFUL::FUL-GFP ful* plants and processed as described in refs. ^{45,46}. Primer sequences used for ChIP-qPCR are detailed in Supplementary Table 2.

EMSA experiment. EMSA was performed as previously described⁴⁷. The sequences of the probes used are detailed in Supplementary Table 2.

AHL clade-A gene family data retrieval. Nucleotide and amino acid sequences for AHL clade-A genes in *A. thaliana* (*AtAHLs*) were retrieved by Biomart from Ensembl Plants (plants.ensembl.org/index.html). For our study we selected 15 additional species from three major plant families—Brassicaceae, Solanaceae and Fabaceae. Initially more species were included, but some were excluded from the analysis (for example, *A. alpina*) for reasons described below. The amino acid sequences of *A. thaliana*, *A. lyrata*, *B. oleracea*, *Brassica rapa*, *Solanum lycopersicum*, *Solanum tuberosum*, *M. trunculata* and *Glycine max* were downloaded from Ensembl Plants ([ftp://ftp.ensemblgenomes.org/](http://ftp.ensemblgenomes.org/)). The genomes of *N. tabacum*, *Capsicum annuum* and *Brassica napus* were downloaded from NCBI Genome (<http://ftp.ncbi.nih.gov/genomes/>), and the genomes of *Phaseolus vulgaris*, *Capsella rubella*, *Capsella grandiflora*, *Boechera stricta* and *Eutrema salsugineum* were downloaded from Phytozome (<https://phytozome.jgi.doe.gov/pz/portal.html>).

Building of profile hidden Markov models (HMMs) and hmmer searches.

Whole-protein sequences of *Arabidopsis* AHL clade-A genes were used as a query, and BLASTP⁴⁸ with an *e*-value set at 0.001 was used to search for AHL clade-A genes in the remaining plant genomes. Only BLASTP hits with >70% coverage and 70% sequence identity and with an intact single AT-hook motif and PPC domain were used for building of profile HMMs. We used MAFFT software⁴⁹ with the FF-NS-i algorithm for construction of seed alignments, which were manually inspected to remove any doubtful sequences. To increase the specificity of the search, columns with many gaps or low conservation were excluded using the trimAl software⁵⁰. We applied a strict non-gap percentage threshold of 80 or similarity score <0.001 such that at least 30% of the columns was conserved. At this point several species were excluded (for example, *A. alpina*) because of extensive gaps in the sequence alignment. Profile HMMs were built from multiple sequence alignment-aligned fasta files using hmmbuild, and subsequent searches against the remaining 16 genomes were carried out using hmmsearch from the HMMER 3.1b1 package⁵¹. AHL proteins in plants consist of two closely resembling clades—clade A and clade B. AHL sequences were classified to the clade-A family based on a comparison with clade-B AHL sequences, where a hit with lower *e*-value for either clade A or clade B would correctly place the sequence in the corresponding clade (for example, a low *e*-value for clade A would place the sequence in clade A and vice versa).

Phylogenetic reconstruction and reconciliation. Phylogenetic analysis was carried out using both maximum likelihood with PhyML⁵² and Bayesian inference implementing the Markov chain Monte Carlo algorithm with MrBayes⁵³. For Bayesian inference, we specified the number of substitution types (nst) equal to 6 and the rate variation (rates) as invgamma. Invgamma states that a proportion of the sites is invariable while the rate for the remaining sites is drawn from a gamma distribution. These settings are equivalent to the GTR+I+gamma model. Two independent analyses (nruns=2) of four chains (three heated and one cold) were run simultaneously for at least 10 million generations, sampling every 1,000 generations. Burn-in was set at 25%. For clade-A AHLs the simulations were run for 10 million generations, sampling every 1,000 generations and convergence was reached at 0.016. For maximum likelihood analysis, we used the default amino acid substitution model LG and the number of bootstrap replicates was specified as 100.

Tree resolving, rearrangement and reconciliation were carried out using NOTUNG software⁵⁴. NOTUNG uses duplication/loss parsimony to fit a gene (protein) tree to a species tree. The species tree was obtained using PhyloT (<https://phylo.t.biobyte.de/>), which generates phylogenetic trees based on NCBI taxonomy. Tree editing/manipulations were performed using the R packages APE⁵⁵ and GEIGER⁵⁶. We applied a strict threshold for rearrangement of 90%, after which we performed reconciliation of the gene (protein) tree with the species tree.

Reconstruction of evolutionary scenario using Dollo parsimony method. Dollo parsimony principles are commonly exploited for two-state character traits. To classify branches as either gene losses or gene gains, we used the Dollo parsimony method which allows for unambiguous reconstruction of ancestral character states, because it is based on the assumption that a complex character that has been lost during evolution of a particular lineage cannot be regained.

Reporting Summary. Further information on research design is available in the Nature Research Reporting Summary linked to this article.

Data availability

All processed data are contained in the manuscript, the Extended Data or the Supplementary Information. Raw data and materials generated during this study are available upon reasonable request.

Received: 19 May 2019; Accepted: 11 March 2020;

Published online: 13 April 2020

References

- Grbić, V. & Bleecker, A. B. Axillary meristem development in *Arabidopsis thaliana*. *Plant J.* **21**, 215–223 (2000).
- Wang, B., Smith, S. M. & Li, J. Genetic regulation of shoot architecture. *Ann. Rev. Plant Biol.* **69**, 437–468 (2018).
- Park, S. J., Eshed, Y. & Lippman, Z. B. Meristem maturation and inflorescence architecture—lessons from the Solanaceae. *Curr. Opin. Plant Biol.* **17**, 70–77 (2014).
- Munné-Bosch, S. Do perennials really senesce? *Trends Plant Sci.* **13**, 216–220 (2008).
- Amasino, R. Floral induction and monocarpic versus polycarpic life histories. *Genome Biol.* **10**, 228 (2009).
- Melzer, S. et al. Flowering-time genes modulate meristem determinacy and growth form in *Arabidopsis thaliana*. *Nat. Genet.* **40**, 1489–1492 (2008).
- Kiefer, C. et al. Divergence of annual and perennial species in the Brassicaceae and the contribution of cis-acting variation at *FLC* orthologues. *Mol. Ecol.* **26**, 3437–3457 (2017).
- Zhao, J., Favero, D. S., Peng, H. & Neff, M. M. *Arabidopsis thaliana* AHL family modulates hypocotyl growth redundantly by interacting with each other via the PPC/DUF296 domain. *Proc. Natl Acad. Sci. USA* **110**, E4688–E4697 (2013).
- Street, I. H., Shah, P. K., Smith, A. M., Avery, N. & Neff, M. M. The AT-hook-containing proteins SOB3/AHL29 and ESC/AHL27 are negative modulators of hypocotyl growth in *Arabidopsis*. *Plant J.* **54**, 1–14 (2008).
- Xiao, C., Chen, F., Yu, X., Lin, C. & Fu, Y.-F. Over-expression of an AT-hook gene, *AHL22*, delays flowering and inhibits the elongation of the hypocotyl in *Arabidopsis thaliana*. *Plant Mol. Biol.* **71**, 39–50 (2009).
- Ng, K.-H., Yu, H. & Ito, T. AGAMOUS controls *GIANT KILLER*, a multifunctional chromatin modifier in reproductive organ patterning and differentiation. *PLoS Biol.* **7**, e1000251 (2009).
- Yun, J., Kim, Y.-S., Jung, J.-H., Seo, P. J. & Park, C.-M. The AT-hook motif-containing protein AHL22 regulates flowering initiation by modifying *FLOWERING LOCUS T* chromatin in *Arabidopsis*. *J. Biol. Chem.* **287**, 15307–15316 (2012).
- Andrés, F. & Coupland, G. The genetic basis of flowering responses to seasonal cues. *Nat. Rev. Genet.* **13**, 627–639 (2012).
- Ko, J., Han, K., Park, S. & Yang, J. Plant body weight-induced secondary growth in *Arabidopsis* and its transcription phenotype revealed by whole-transcriptome profiling. *Plant Physiol.* **135**, 1069–1083 (2004).
- Bergonzi, S. et al. Mechanisms of age-dependent response to winter temperature in perennial flowering of *Arabidopsis alpina*. *Science* **340**, 1094–1097 (2013).
- Zhou, C.-M. et al. Molecular basis of age-dependent vernalization in *Cardamine flexuosa*. *Science* **340**, 1097–1100 (2013).
- Lee, J. & Lee, I. Regulation and function of SOC1, a flowering pathway integrator. *J. Exp. Bot.* **61**, 2247–2254 (2010).
- Immink, R. G. H. et al. Characterization of SOC1's central role in flowering by the identification of its upstream and downstream regulators. *Plant Physiol.* **160**, 433–449 (2012).
- Tao, Z. et al. Genome-wide identification of SOC1 and SVP targets during the floral transition in *Arabidopsis*. *Plant J.* **70**, 549–561 (2012).
- Matsoukas, I. G., Massiah, A. J. & Thomas, B. Florigenic and antiflorigenic signaling in plants. *Plant Cell Physiol.* **53**, 1827–1842 (2012).
- Turnbull, C. Long-distance regulation of flowering time. *J. Exp. Bot.* **62**, 4399–43413 (2011).
- Song, Y. H., Ito, S. & Imaizumi, T. Flowering time regulation: photoperiod- and temperature-sensing in leaves. *Trends Plant Sci.* **18**, 575–583 (2013).
- Andrés, F. et al. SHORT VEGETATIVE PHASE reduces gibberellin biosynthesis at the *Arabidopsis* shoot apex to regulate the floral transition. *Proc. Natl Acad. Sci. USA* **111**, E2760–E2769 (2014).
- Yu, S. et al. Gibberellin regulates the *Arabidopsis* floral transition through miR156-targeted *SQUAMOSA* promoter binding-like transcription factors. *Plant Cell* **24**, 3320–3332 (2012).
- Wang, J. W. Regulation of flowering time by the miR156-mediated age pathway. *J. Exp. Bot.* **5**, 4723–4730 (2014).
- Matsushita, A., Furumoto, T., Ishida, S. & Takahashi, Y. AGF1, an AT-hook protein, is necessary for the negative feedback of *AtGA3ox1* encoding GA 3-oxidase. *Plant Physiol.* **143**, 1152–1162 (2007).
- Huang, S. et al. Overexpression of *20-Oxidase* confers a gibberellin-overproduction phenotype in *Arabidopsis*. *Plant Physiol.* **118**, 773–781 (1998).
- Rieu, I. et al. The gibberellin biosynthetic genes *AtGA20ox1* and *AtGA20ox2* act, partially redundantly, to promote growth and development throughout the *Arabidopsis* life cycle. *Plant J.* **53**, 488–504 (2008).
- Tilmes, V. et al. Gibberellins act downstream of Arabidopsis *PERPETUAL FLOWERING1* to accelerate floral induction during vernalization. *Plant Physiol.* **180**, 1549–1563 (2019).
- Zhao, J., Favero, D. S., Qiu, J., Roalson, E. H. & Neff, M. M. Insights into the evolution and diversification of the AT-hook Motif Nuclear Localized gene family in land plants. *BMC Plant Biol.* **14**, 266 (2014).
- Remington, D. L., Figueroa, J. & Rane, M. Timing of shoot development transitions affects degree of perennality in *Arabidopsis lyrata* (Brassicaceae). *BMC Plant Biol.* **15**, 1–13 (2015).
- Lim, P. O. et al. Overexpression of a chromatin architecture-controlling AT-hook protein extends leaf longevity and increases the post-harvest storage life of plants. *Plant J.* **52**, 1140–1153 (2007).
- Dekker, J., Marti-Renom, M. A. & Mirny, L. A. Exploring the three-dimensional organization of genomes: interpreting chromatin interaction data. *Nat. Rev. Genet.* **14**, 390–403 (2013).
- Wang, J.-W., Czech, B. & Weigel, D. miR156-regulated *SPL* transcription factors define an endogenous flowering pathway in *Arabidopsis thaliana*. *Cell* **138**, 738–749 (2009).
- Karimi, M., Depicker, A. & Hilson, P. Recombinational cloning with plant gateway vectors. *Plant Physiol.* **145**, 1144–1154 (2007).
- Passarinho, P. et al. BABY BOOM target genes provide diverse entry points into cell proliferation and cell growth pathways. *Plant Mol. Biol.* **68**, 225–237 (2008).
- Becker, D., Kemper, E., Schell, J. & Masterson, R. New plant binary vectors with selectable markers located proximal to the left T-DNA border. *Plant Mol. Biol.* **20**, 1195–1197 (1992).
- Den Dulk-Ras, A. & Hooykaas J. P. Electroporation of *Agrobacterium tumefaciens*. *Methods Mol. Biol.* **55**, 63–72 (1995).
- Clough, S. J. & Bent, A. F. Floral dip: a simplified method for *Agrobacterium*-mediated transformation of *Arabidopsis thaliana*. *Plant J.* **16**, 735–743 (1998).
- Baltes, N. J., Gil-Humanes, J., Cermak, T., Atkins, P. & Voytas, D. F. DNA replicons for plant genome engineering. *Plant Cell* **26**, 151163 (2014).
- Murashige, T. & Skoog, F. A revised medium for rapid growth and bio assays with tobacco tissue cultures. *Physiol. Plant.* **15**, 473–497 (1962).
- Doyle, J. J. Isolation of plant DNA from fresh tissue. *Focus* **12**, 13–15 (1990).
- Anandalakshmi, R. et al. A viral suppressor of gene silencing in plants. *Proc. Natl Acad. Sci. USA* **95**, 13079–13084 (1998).
- Pfaffl, M. W. A new mathematical model for relative quantification in real-time RT-PCR. *Nucleic Acids Res.* **29**, e45 (2001).
- Mourik, H. Van, Muiño, J. M., Pajoro, A., Angenent, G. C. & Kaufmann, K. Characterization of *in vivo* DNA-binding events of plant transcription factors by ChIP-seq: experimental protocol and computational analysis. *Methods Mol. Biol.* **1284**, 93–121 (2015).
- Balanza, V. et al. Genetic control of meristem arrest and life span in *Arabidopsis* by a FRUITFULL-APETALA2 pathway. *Nat. Commun.* **9**, 565 (2018).

47. Bemer, M. et al. FRUITFULL controls *SAUR10* expression and regulates *Arabidopsis* growth and architecture. *J. Exp. Bot.* **68**, 3391–3403 (2017).
48. Altschup, S. F., Gish, W., Pennsylvania, T. & Park, U. Basic local alignment search tool. *J. Mol. Biol.* **215**, 403–410 (1990).
49. Katoh, K., Misawa, K., Kuma, K. & Miyata, T. MAFFT: a novel method for rapid multiple sequence alignment based on fast Fourier transform. *Nucleic Acids Res.* **30**, 3059–3066 (2002).
50. Capella-gutiérrez, S., Silla-martínez, J. M. & Gabaldón, T. TrimAl: a tool for automated alignment trimming in large-scale phylogenetic analyses. *Bioinformatics* **25**, 1972–1973 (2009).
51. Eddy, S. R. Accelerated profile HMM searches. *PLoS Comp. Biol.* **7**, e1002195 (2011).
52. Guindon, S. & Gascuel, O. A simple, fast, and accurate algorithm to estimate large phylogenies by maximum likelihood. *Syst. Biol.* **5**, 696–704 (2003).
53. Ronquist, F. & Huelsenbeck, J. P. MrBayes 3: Bayesian phylogenetic inference under mixed models. *Bioinformatics* **19**, 1572–1574 (2003).
54. Liebert, M. A., Chen, K., Durand, D., Farach-colton, M. & Al, C. E. T. NOTUNG: a program for dating gene duplications. *J. Comp. Biol.* **7**, 429–447 (2000).
55. Paradis, E., Claude, J. & Strimmer, K. APE: analyses of phylogenetics and evolution in R language. *Bioinformatics* **20**, 289–290 (2004).
56. Harmon, L. J. et al. GEIGER: investigating evolutionary radiations. *Bioinformatics* **24**, 129–131 (2008).

Acknowledgements

We thank K. Boutilier and T. Greb for critical comments on the manuscript. O.K. was financially supported by a grant from the Iran Ministry of Science, Research and Technology (no. 89100156), and subsidies were provided by Generade and the Building Blocks of Life research programme (no. 737.016.013, to R.O.), which is (partly) financed by the Dutch Research Council (NWO). M.K. was financially supported by a fellowship of the Institute of Biotechnology & Genetic Engineering at the Agricultural University

of Peshawar with financial support by the Higher Education Commission of Pakistan. R.R.H. was financially supported by the KU Leuven Research Fund. M.B. was supported by grant no. ALWOP.199, which is (partly) financed by NWO. P.M. and M.C. were supported in part by Innovation Subsidy Collaborative Projects (no. IS054064) from the Dutch Ministry of Economic Affairs.

Author contributions

O.K. and R.O. conceived and supervised the project. All authors designed the experiments and analysed and interpreted the results. O.K. and A.R. performed the majority of the *Arabidopsis* experiments, with contributions from M.B., P.M. and M.C. M.K. generated and analysed the tobacco lines. R.R.H. and V.N. analysed the *AHL* gene families in mono- and polycarpic plant species. O.K. and R.O. wrote the manuscript. All authors read and commented on versions of the manuscript.

Competing interests

The authors declare no competing interests.

Additional information

Extended data is available for this paper at <https://doi.org/10.1038/s41477-020-0637-z>.

Supplementary information is available for this paper at <https://doi.org/10.1038/s41477-020-0637-z>.

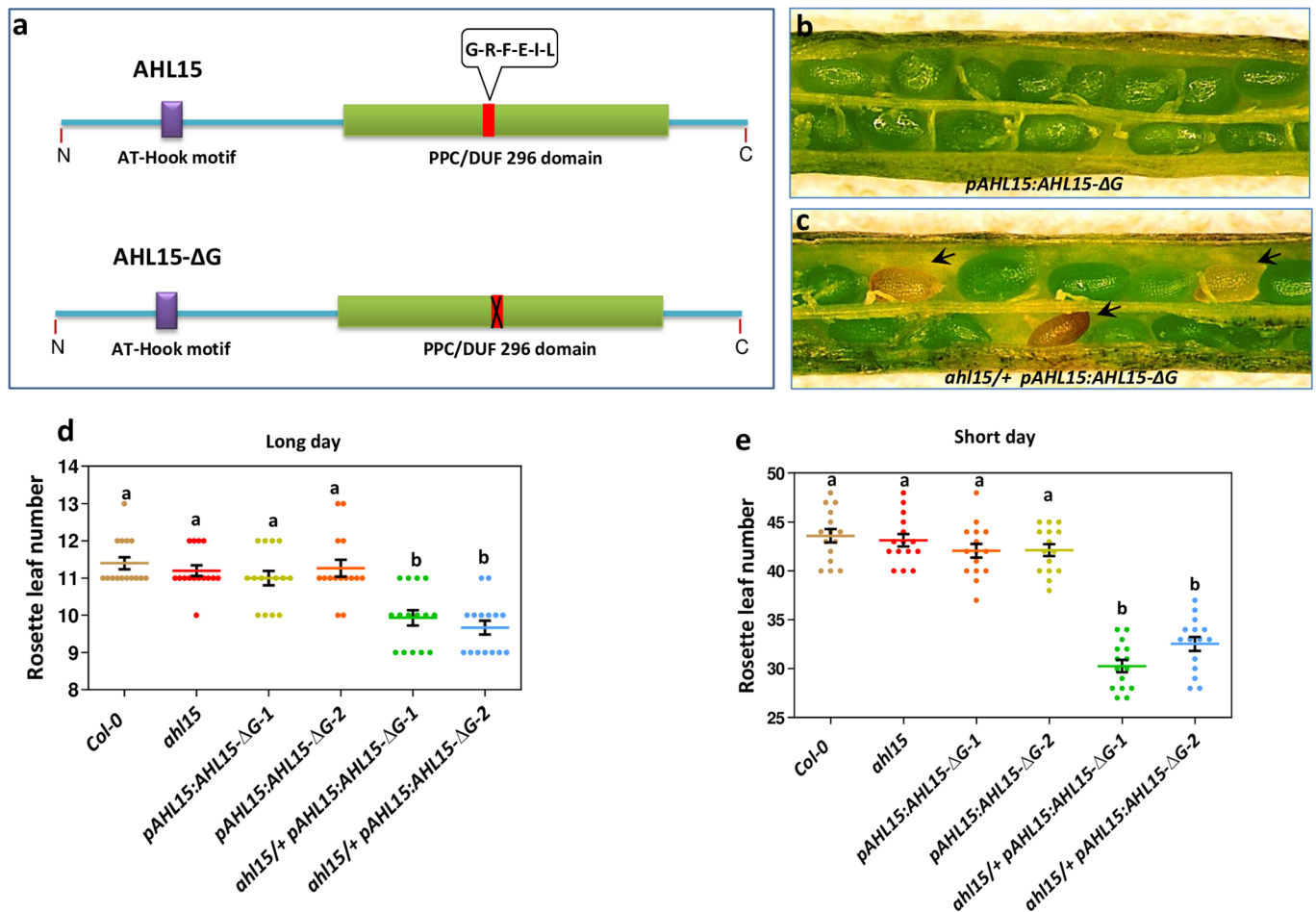
Correspondence and requests for materials should be addressed to R.O.

Peer review information *Nature Plants* thanks Richard Amasino and the other, anonymous, reviewers for their contribution to the peer review of this work.

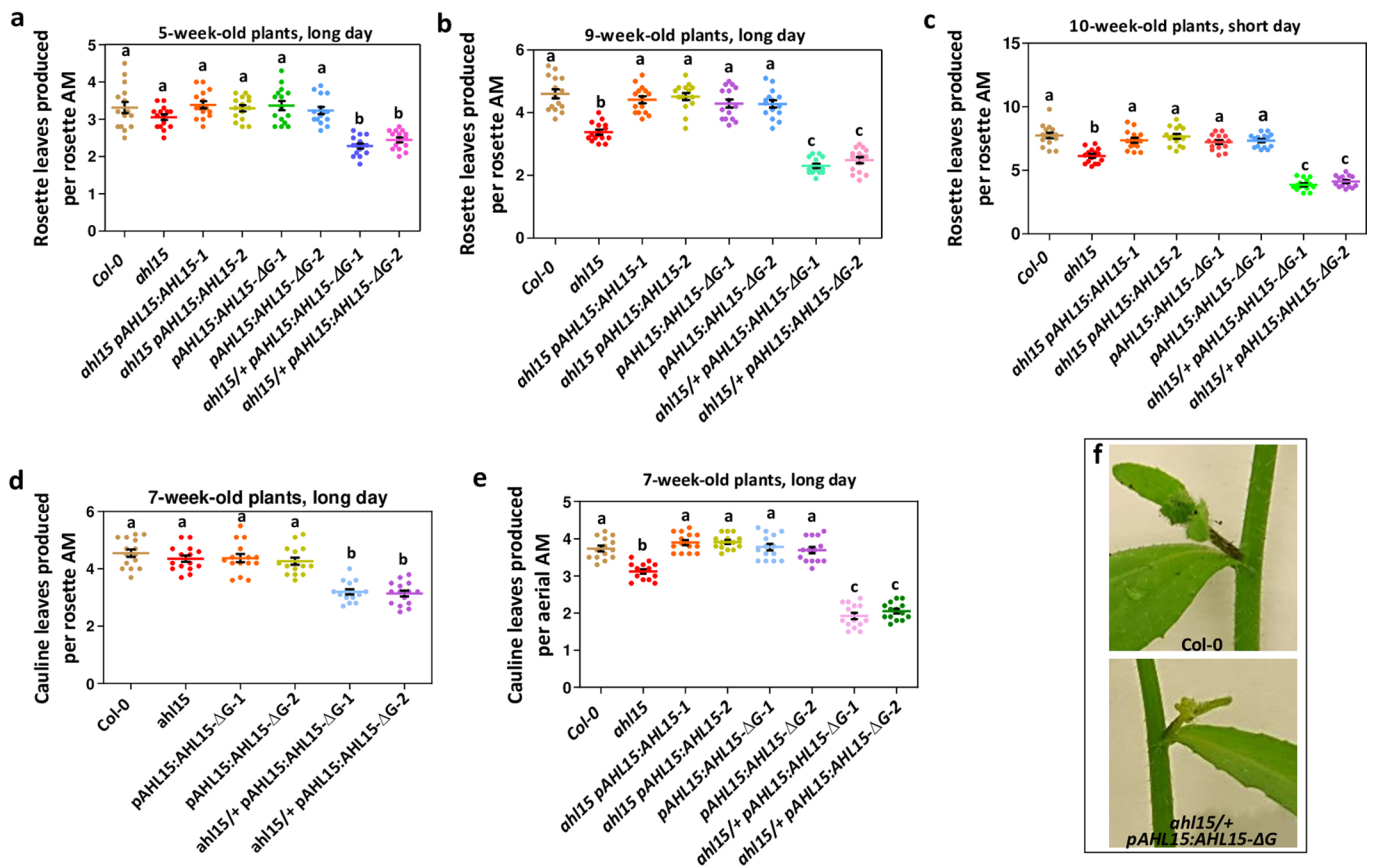
Reprints and permissions information is available at www.nature.com/reprints.

Publisher's note Springer Nature remains neutral with regard to jurisdictional claims in published maps and institutional affiliations.

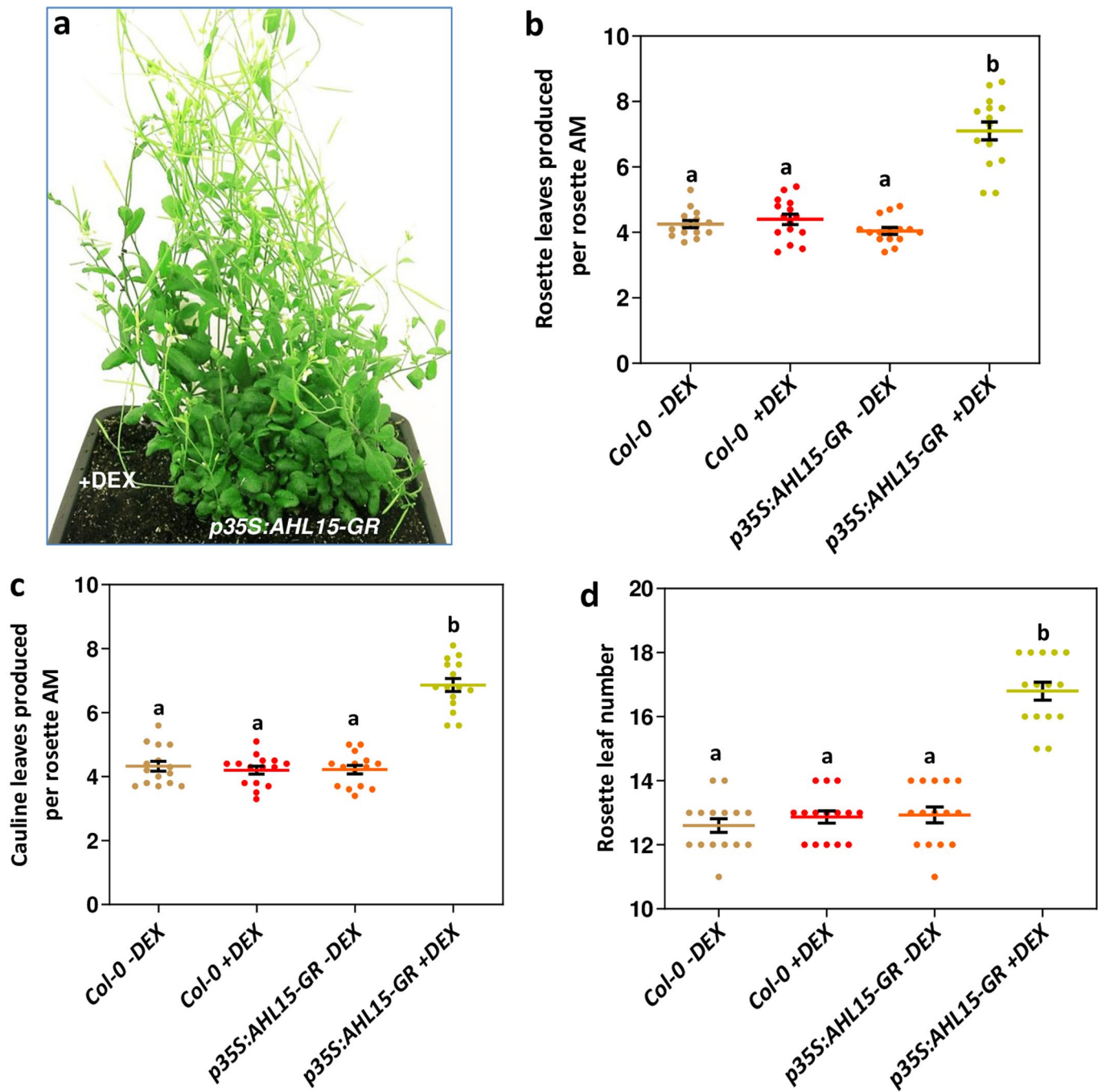
© The Author(s), under exclusive licence to Springer Nature Limited 2020



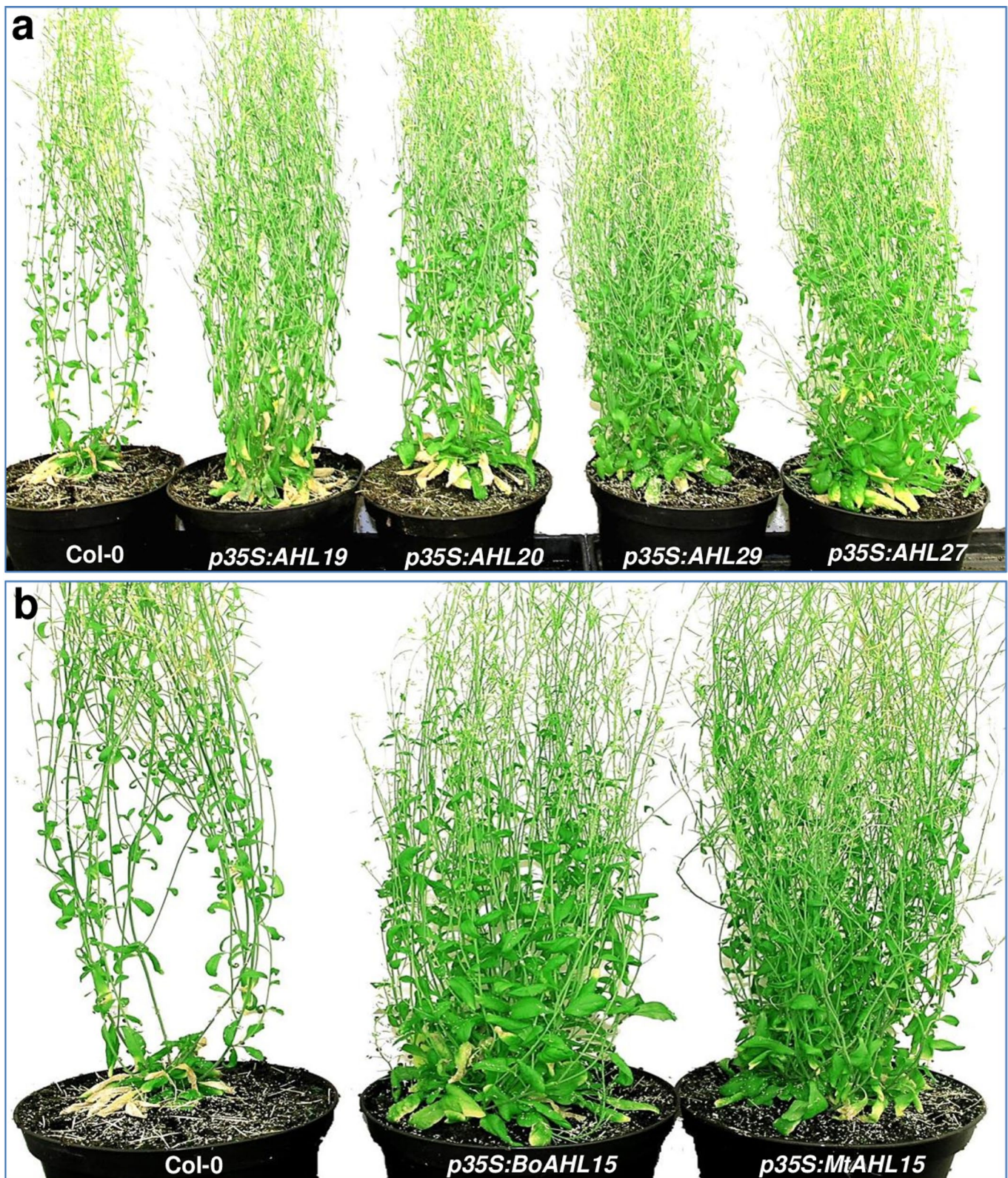
Extended Data Fig. 1 | Expression of a dominant negative AHL15-ΔG mutant protein. Expression of a dominant negative AHL15-ΔG mutant protein in the *Arabidopsis* *ah15* mutant background causes early flowering and impairs seed development. **a**. The schematic domain structure of AHL15 and the dominant negative AHL15-ΔG version, in which six-conserved amino-acids (Gly-Arg-Phe-Glu-Ile-Leu, red box) are deleted from the C-terminal PPC domain. **b**. Wild-type seed development in *pAHL15:AHL15-ΔG* siliques. **c**. Aberrant seed development (arrowheads) in *ah15/+ pAHL15:AHL15-ΔG* siliques (observed in 3 independent *pAHL15:AHL15-ΔG* lines crossed with the *ah15* mutant). Similar results were obtained in three independent experiments. **d**, **e**. The number of rosette leaves produced by the SAM in wild-type, *ah15*, *pAHL15:AHL15-ΔG* and *ah15/+ pAHL15:AHL15-ΔG* plants grown in long day (LD, **d**) or short day (SD, **e**) conditions. Two independent transgenic lines (1 and 2) were used in each experiment. Dots in **d** and **e** indicate the rosette leaf number per plant ($n=15$ biologically independent plants), horizontal lines the mean and error bars the s.e.m. Letters (a, b, c) indicate statistically significant differences ($P < 0.01$), as determined by a one-way ANOVA with a Tukey's HSD post hoc test. The P values can be found in the Supplementary Tables 6 and 7.



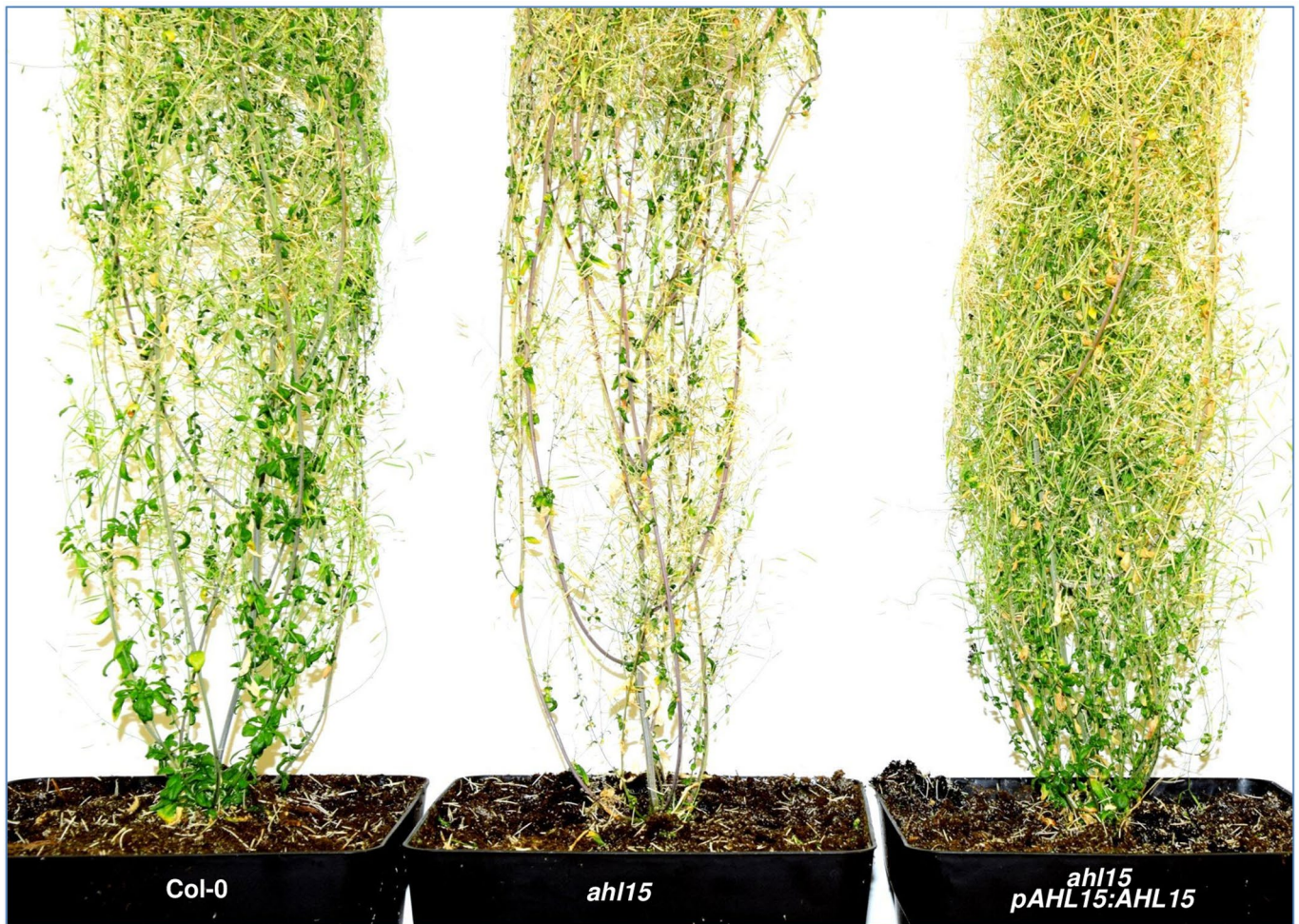
Extended Data Fig. 2 | AHL15 and other clade A AHL genes represses AM maturation in Arabidopsis. **a, b.** The number of rosette leaves produced per rosette AM of wild-type, *ahl15*, *ahl15 pAHL15:AHL15*, *pAHL15:AHL15-ΔG* and *ahl15/+ pAHL15:AHL15-ΔG* plants 5 (**a**), 9 (**b**), or 10 weeks (**c**) after germination in long day (LD, **a,b**) or short day (SD, **c**) conditions. **d, e.** The number of cauline leaves produced by rosette AMs (**d**) or by aerial AMs (**e**) of 7-week-old wild-type, *ahl15*, *ahl15 pAHL15:AHL15*, *pAHL15:AHL15-ΔG* and *ahl15/+ pAHL15:AHL15-ΔG* plants. Dots in a-e indicate rosette or cauline leaf number per AM per plant ($n=15$ biologically independent plants), horizontal lines the mean, and error bars the s.e.m. Letters (a, b, c) indicate statistically significant differences ($P < 0.01$), as determined by a one-way ANOVA with a Tukey's HSD post hoc test. The P values are provided in Supplementary Tables 8–12. **f.** A lateral inflorescence with cauline leaves formed on the first inflorescence node of a wild-type (top) or *ahl15/+ pAHL15:AHL15-ΔG* plant (bottom). Similar results were obtained in three independent experiments.



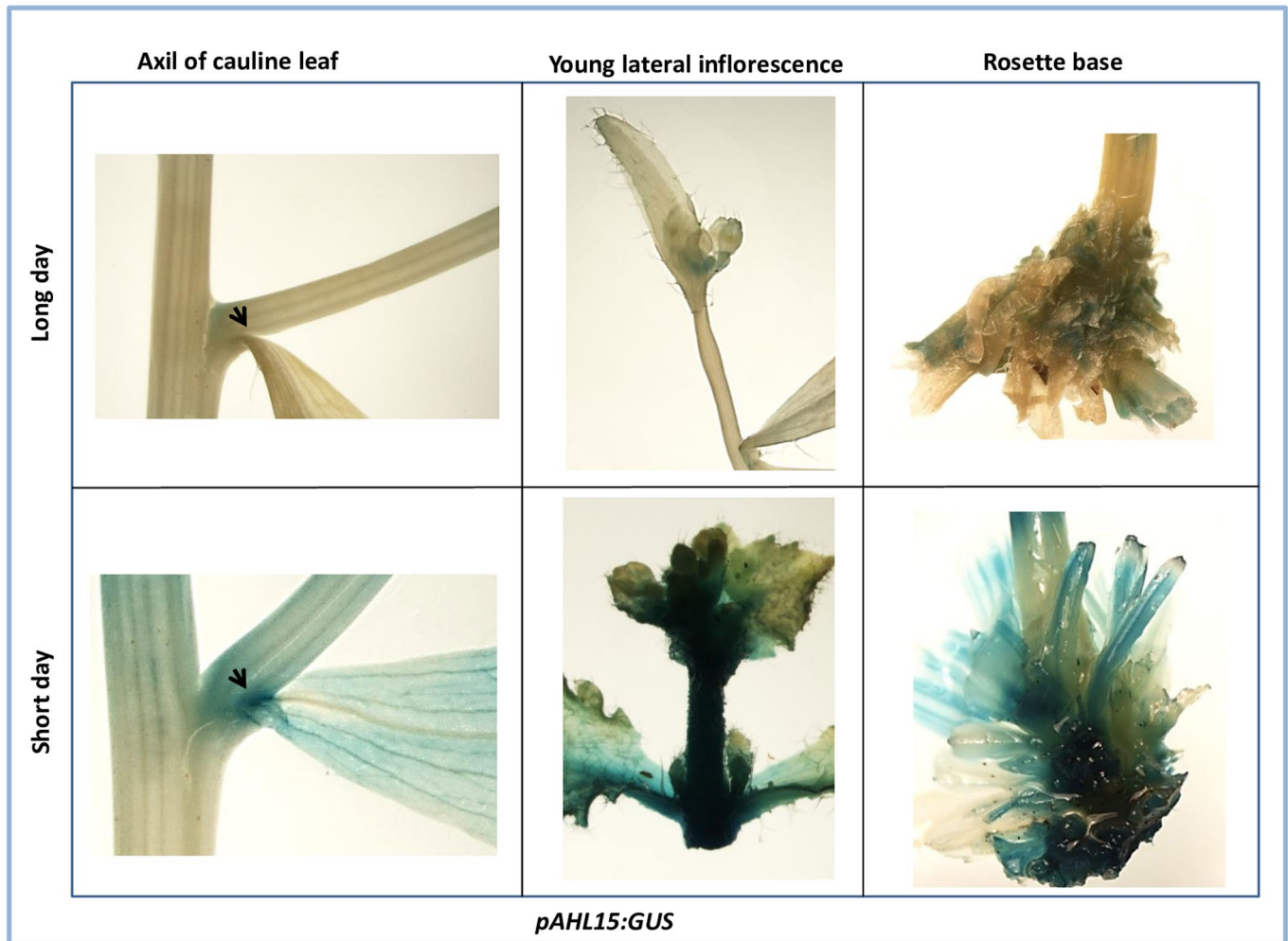
Extended Data Fig. 4 | *AHL15* overexpression delays floral transition of the SAM and represses AM maturation. a. Shoot phenotype of a flowering 7-week-old *35S:AHL15-GR* plant that was DEX-treated upon bolting (5 weeks old). Similar results were obtained in four independent experiments. **b, c.** Number of rosette leaves (**b**) or cauline leaves (**c**) produced by rosette AMs of 7-week-old mock-treated wild-type, DEX-treated wild-type, mock-treated *35S:AHL15-GR* and DEX-treated *35S:AHL15-GR* plants. Plants were DEX-treated upon bolting (5 weeks old) and scored 2 weeks later. **d.** The number of rosette leaves produced by the SAM in mock-treated wild-type, DEX-treated wild-type, mock-treated *35S:AHL15-GR* and DEX-treated *35S:AHL15-GR* plants. Non-flowering (3-week-old) plants were treated and the SAM-produced rosette leaves were counted after bolting. Dots in **b-d** indicate number of leaves (per AM or SAM) per plant ($n=15$ biologically independent plants), horizontal lines the mean, and error bars the s.e.m. Letters (a, b, c) indicate statistically significant differences ($P < 0.01$), as determined by a one-way ANOVA with a Tukey's HSD post hoc test. The P values are provided in Supplementary Tables 13–15. Plants were grown in LD conditions.



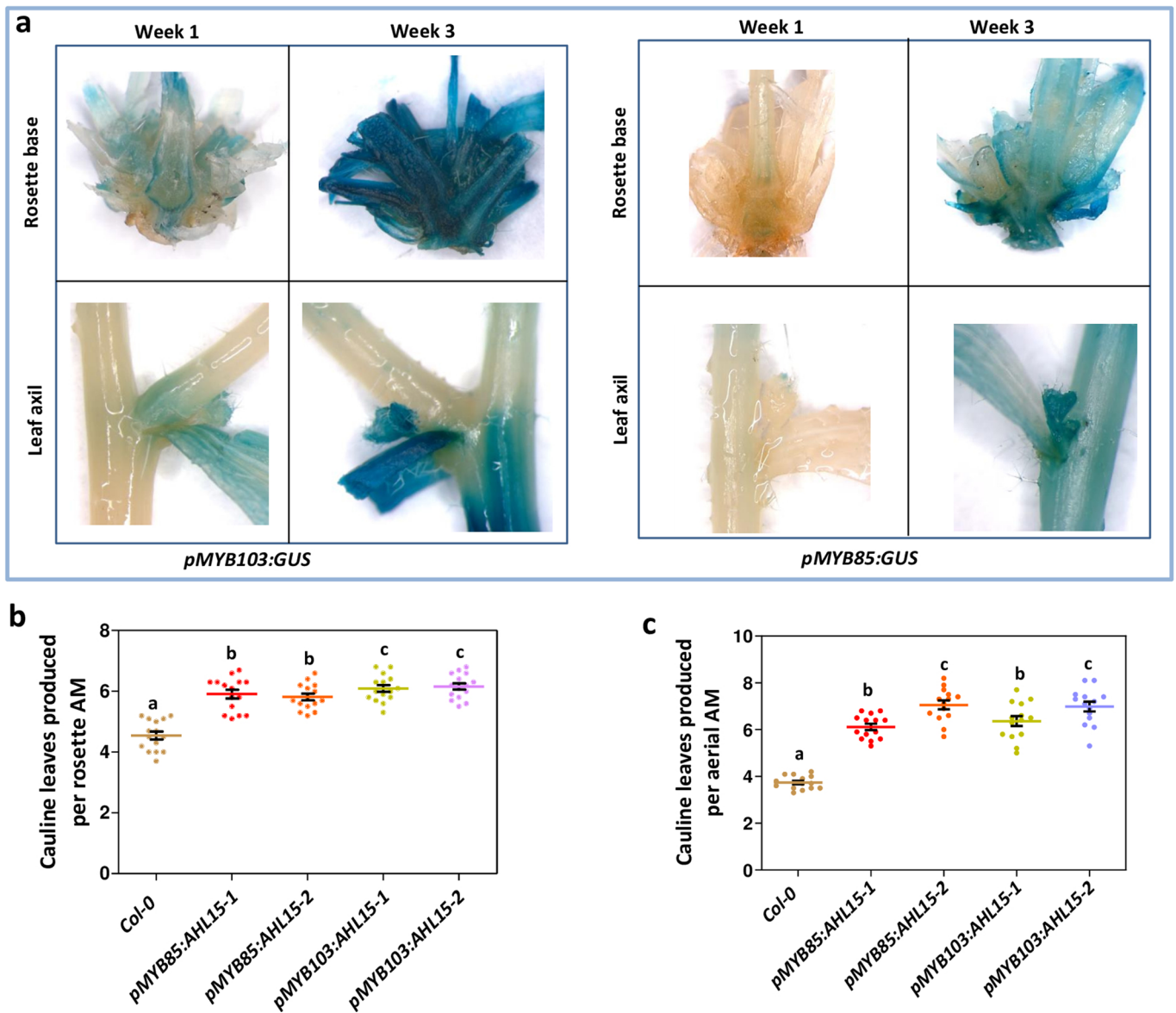
Extended Data Fig. 5 | Overexpression of *Arabidopsis* AHL15 paralogs or putative orthologs represses AM maturation in *Arabidopsis*. Overexpression of *Arabidopsis* AHL15 paralogs or putative orthologs represses AM maturation in *Arabidopsis*. (**a** and **b**) Wild-type (Col-0) or transgenic 7-week-old *Arabidopsis* plants overexpressing *Arabidopsis* AHL19, AHL20, AHL27 and AHL29 (**a**), or the putative AHL15 orthologs from *Brassica oleracea* (BoAHL15) or *Medicago truncatula* (MtAHL15) (**b**). For **a** and **b** similar results were obtained in two independent experiments. Plants were grown in LD conditions. For presentation purposes, the original background of the images was replaced by a homogeneous white background.



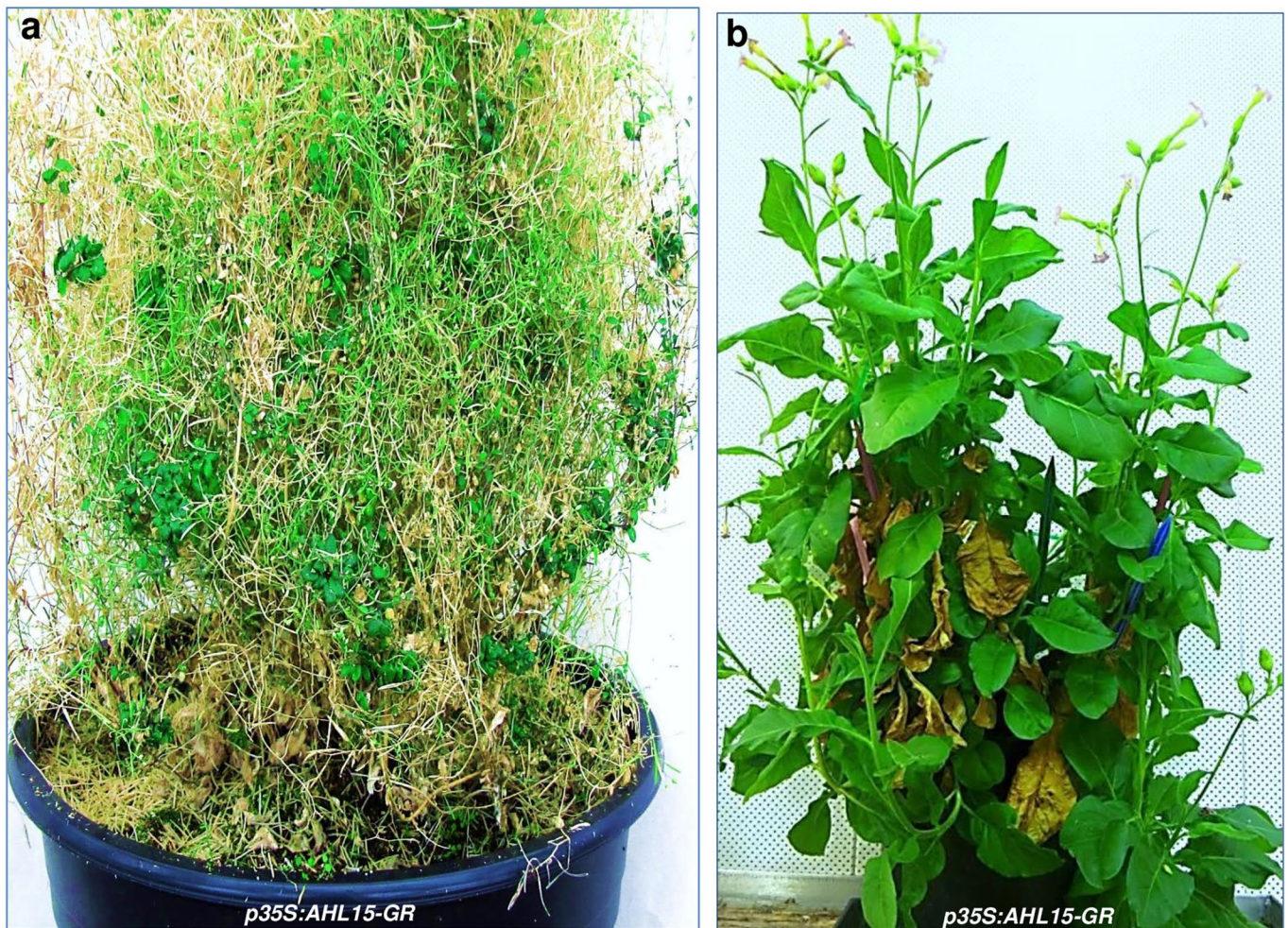
Extended Data Fig. 6 | *AHL15* enhances the longevity of short day-grown *Arabidopsis* plants. Phenotype of 5-month-old wild-type (Col-0, left), *ah15* (middle) and *ah15 pAHL15:AHL15* (right) plants. The plants were grown in SD conditions. Similar results were obtained in two independent experiments. For presentation purposes, the original background of the image in was replaced by a homogeneous white background.



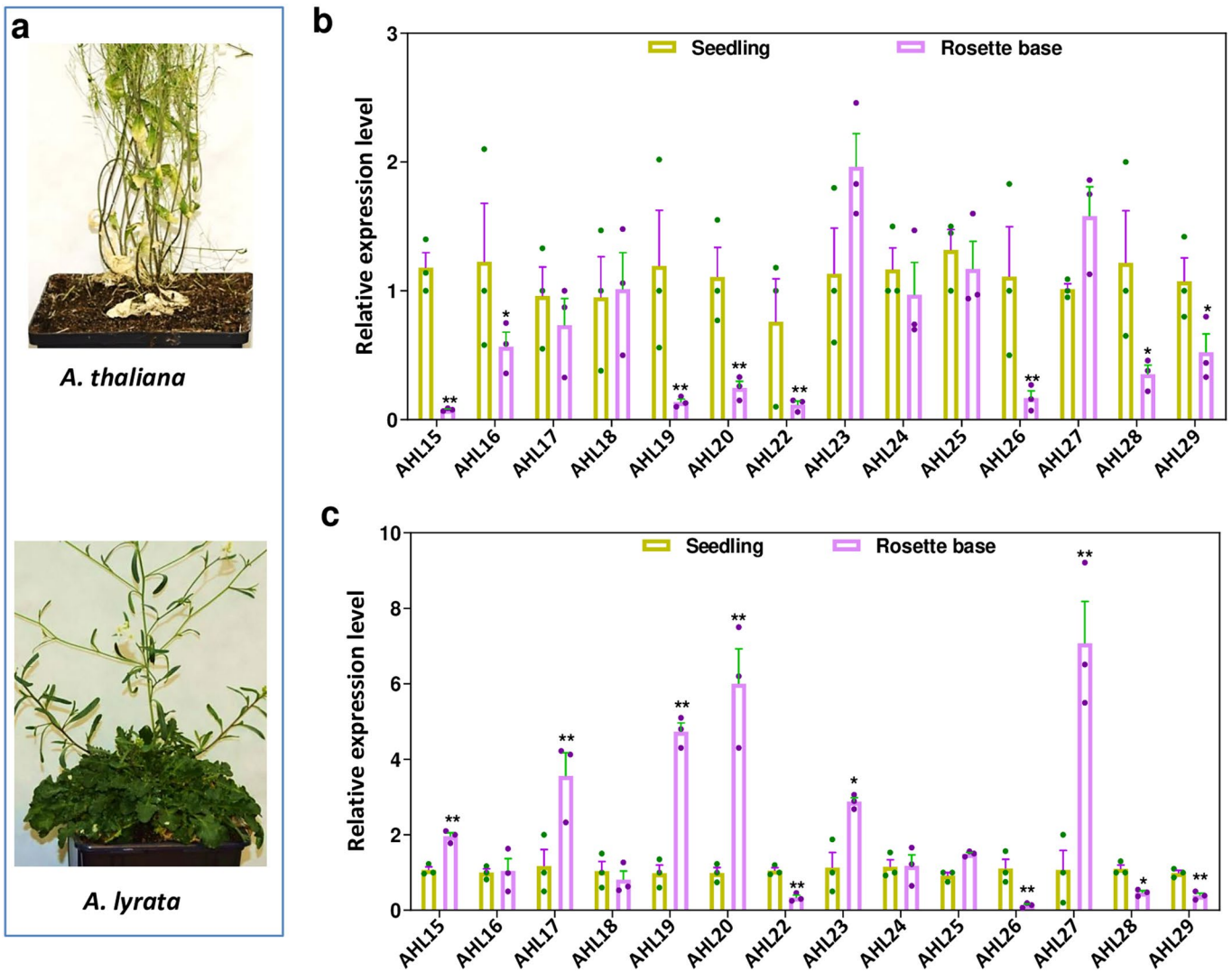
Extended Data Fig. 7 | *AHL15* expression is day length sensitive. Expression of the *pAHL15:GUS* reporter in the axil of a cauline leaf (left, arrowheads), Young lateral inflorescence (middle) and rosette base (right) of a 9-week-old plant grown in LD conditions (top) or a 4-month-old plant grown under SD conditions (bottom). Similar results were obtained in two independent experiments.



Extended Data Fig. 8 | *AHL15* overexpression in the rosette base and leaf axils delays AM maturation in *Arabidopsis*. **a**, Expression of *pMYB85:GUS* and *pMYB103:GUS* reporters in the rosette base (top) or leaf axils (bottom) of *Arabidopsis* plants respectively one or three weeks after flowering, as monitored by histochemical GUS staining. Similar results were obtained in two independent experiments. **b, c**, The number of cauline leaves produced by rosette AMs (**b**) or aerial AMs (**c**) of 6-week-old (**b**) or 7-week-old (**c**) wild-type, *pMYB85:AHL15* or *pMYB103:AHL15* plants grown in LD conditions. Dots in **b** and **c** indicate number of cauline leaves produced per AM per plant ($n=15$ biologically independent plants), horizontal lines indicate the mean, and error bars the s.e.m. Letters (a, b, c) indicate statistically significant differences ($P < 0.01$), as determined by a one-way ANOVA with a Tukey's HSD post hoc test. The P values can be found in Supplementary Tables 16 and 17.



Extended Data Fig. 9 | *AHL15* overexpression promotes longevity in *Arabidopsis* and tobacco. **a. Renewed vegetative growth on aerial branches of a 5-month-old *Arabidopsis* 35S:*AHL15-GR* plant, 4 weeks after spraying with 20 μ M DEX. Similar results were obtained in three independent experiments. **b.** Efficient production of leaves and inflorescences in a 3-year-old 35S:*AHL15-GR* tobacco plant, 3 weeks after treatment with 30 μ M DEX, following 6 previous cycles of DEX-induced seed production. Similar results were obtained in two independent experiments. Plants in **a** and **b** were grown in LD conditions.**



Extended Data Fig. 10 | Expression of clade-A AHL genes in seedlings or in the rosette base of flowering *Arabidopsis* or *A. lyrata* plants. **a**, Shoot phenotype of a 3-month-old *Arabidopsis* (upper panel) or a 4-month-old *A. lyrata* (lower panel) plant grown in LD conditions. Similar results were obtained in two independent experiments. **b**, **c**, qPCR analysis of the expression of clade-A AHL genes in 2-week-old seedlings or in the rosette base of 2-month-old flowering plants of *A. thaliana* (**b**) or *A. lyrata* (**c**). Dots in **b** and **c** indicate relative expression levels per experiment ($n=3$ biologically independent replicates), bars indicate the mean, and error bars indicate the s.e.m. Asterisks indicate significant differences from mock-treated plants (* $p<0.05$, ** $p<0.01$, *** $p<0.001$), as determined by a two-sided Student's *t*-test.

Reporting Summary

Nature Research wishes to improve the reproducibility of the work that we publish. This form provides structure for consistency and transparency in reporting. For further information on Nature Research policies, see [Authors & Referees](#) and the [Editorial Policy Checklist](#).

Statistics

For all statistical analyses, confirm that the following items are present in the figure legend, table legend, main text, or Methods section.

n/a Confirmed

- The exact sample size (n) for each experimental group/condition, given as a discrete number and unit of measurement
- A statement on whether measurements were taken from distinct samples or whether the same sample was measured repeatedly
- The statistical test(s) used AND whether they are one- or two-sided
Only common tests should be described solely by name; describe more complex techniques in the Methods section.
- A description of all covariates tested
- A description of any assumptions or corrections, such as tests of normality and adjustment for multiple comparisons
- A full description of the statistical parameters including central tendency (e.g. means) or other basic estimates (e.g. regression coefficient) AND variation (e.g. standard deviation) or associated estimates of uncertainty (e.g. confidence intervals)
- For null hypothesis testing, the test statistic (e.g. F , t , r) with confidence intervals, effect sizes, degrees of freedom and P value noted
Give P values as exact values whenever suitable.
- For Bayesian analysis, information on the choice of priors and Markov chain Monte Carlo settings
- For hierarchical and complex designs, identification of the appropriate level for tests and full reporting of outcomes
- Estimates of effect sizes (e.g. Cohen's d , Pearson's r), indicating how they were calculated

Our web collection on [statistics for biologists](#) contains articles on many of the points above.

Software and code

Policy information about [availability of computer code](#)

Data collection

Biomart v0.9, BlastP 2.10,

Data analysis

MAFFT7.4, trimAL1.2, HMMER3.1b1, PhyML3.0, MrBayes3.2.7, NOTUNG2.9, PhyloT, R packages APE5.3 and GEIGER2.0

For manuscripts utilizing custom algorithms or software that are central to the research but not yet described in published literature, software must be made available to editors/reviewers. We strongly encourage code deposition in a community repository (e.g. GitHub). See the Nature Research [guidelines for submitting code & software](#) for further information.

Data

Policy information about [availability of data](#)

All manuscripts must include a [data availability statement](#). This statement should provide the following information, where applicable:

- Accession codes, unique identifiers, or web links for publicly available datasets
- A list of figures that have associated raw data
- A description of any restrictions on data availability

All data generated or analysed during this study are included in this published article (and its supplementary information files).

Field-specific reporting

Please select the one below that is the best fit for your research. If you are not sure, read the appropriate sections before making your selection.

- Life sciences Behavioural & social sciences Ecological, evolutionary & environmental sciences

For a reference copy of the document with all sections, see [nature.com/documents/nr-reporting-summary-flat.pdf](https://www.nature.com/documents/nr-reporting-summary-flat.pdf)

Life sciences study design

All studies must disclose on these points even when the disclosure is negative.

| | |
|-----------------|--|
| Sample size | <input type="text" value="No statistical method was used to determine sample size. Sample size was chosen based on what is common in the field"/> |
| Data exclusions | <input type="text" value="No data have been excluded from our analysis"/> |
| Replication | <input type="text" value="All described experiments were repeated at least once, and appeared reproducible."/> |
| Randomization | <input type="text" value="For plant phenotyping and morphometry, progeny of a genetically homozygous plant parent were randomly selected."/> |
| Blinding | <input type="text" value="Blinding was not relevant in our study, since the phenotypic differences between the different lines were sufficiently large."/> |

Reporting for specific materials, systems and methods

We require information from authors about some types of materials, experimental systems and methods used in many studies. Here, indicate whether each material, system or method listed is relevant to your study. If you are not sure if a list item applies to your research, read the appropriate section before selecting a response.

Materials & experimental systems

- | n/a | Involvement in the study |
|-------------------------------------|--|
| <input type="checkbox"/> | <input checked="" type="checkbox"/> Antibodies, Anti-GFP, see ref. 45/46 |
| <input checked="" type="checkbox"/> | <input type="checkbox"/> Eukaryotic cell lines |
| <input checked="" type="checkbox"/> | <input type="checkbox"/> Palaeontology |
| <input checked="" type="checkbox"/> | <input type="checkbox"/> Animals and other organisms |
| <input checked="" type="checkbox"/> | <input type="checkbox"/> Human research participants |
| <input checked="" type="checkbox"/> | <input type="checkbox"/> Clinical data |

Methods

- | n/a | Involvement in the study |
|-------------------------------------|---|
| <input checked="" type="checkbox"/> | <input type="checkbox"/> ChIP-seq |
| <input checked="" type="checkbox"/> | <input type="checkbox"/> Flow cytometry |
| <input checked="" type="checkbox"/> | <input type="checkbox"/> MRI-based neuroimaging |